HDL-TR-1832
November 1977

(11)

FC

Measurement of the Impulse Response of Communication Antennas

U.S. Army Materiel Development and Readiness Command

HARRY DIAMOND LABORATORIES

Adelphi, Maryland 20783

The findings in this report are not to be construed as an official Department of the Army position unless so designated by other authorized documents.

Citation of manufacturers' or trade names does not constitute an official indorsement or approval of the use thereof.

Destroy this report when it is no longer needed. Do not return it to the originator.

UNCLASSIFIED

SECURITY CLASSIFICATION OF THIS PAGE *(When Data Entered)*

REPORT DOCUMENTATION PAGE

READ INSTRUCTIONS BEFORE COMPLETING FORM

1. REPORT NUMBER: HDL-TR-1832	2. GOVT ACCESSION NO.
3. RECIPIENT'S CATALOG NUMBER	
4. TITLE *(and Subtitle)*: Measurement of the Impulse Response of Communication Antennas,	5. TYPE OF REPORT & PERIOD COVERED: Technical Report,
6. PERFORMING ORG. REPORT NUMBER	
7. AUTHOR(s): Daniel H. Schaubert	8. CONTRACT OR GRANT NUMBER(s): DA: 1W162118AH75
9. PERFORMING ORGANIZATION NAME AND ADDRESS: Harry Diamond Laboratories, 2800 Powder Mill Road, Adelphi, MD 20783	10. PROGRAM ELEMENT, PROJECT, TASK AREA & WORK UNIT NUMBERS: Program Ele: 6.21.18.A
11. CONTROLLING OFFICE NAME AND ADDRESS: US Army Materiel Development and Readiness Command, Alexandria, VA 22333	12. REPORT DATE: Nov 1977
	13. NUMBER OF PAGES: 46
14. MONITORING AGENCY NAME & ADDRESS *(If different from Controlling Office)*: 42 p.	15. SECURITY CLASS. *(of this report)*: UNCLASSIFIED
	15a. DECLASSIFICATION/DOWNGRADING SCHEDULE

16. DISTRIBUTION STATEMENT *(of this Report)*

Approved for public release; distribution unlimited.

17. DISTRIBUTION STATEMENT *(of the abstract entered in Block 20, if different from Report)*

18. SUPPLEMENTARY NOTES

HDL Project: X75615
DRCMS Code: 612118.11.H7500

19. KEY WORDS *(Continue on reverse side if necessary and identify by block number)*

Antenna measurements
Antenna transients
Antenna impulse response
Antenna EMP response

20. ABSTRACT *(Continue on reverse side if necessary and identify by block number)*

A technique for measuring the transient response of uhf and vhf communication antennas is described. The procedure permits accurate determination of the impulse response of linear, time-invariant antennas over the bandwidth of concern for high-altitude EMP. The experimental procedure is easy and inexpensive to implement and is suitable for laboratory and field testing. A key part of the experimental equipment is the

DD FORM 1 JAN 73 1473 EDITION OF 1 NOV 65 IS OBSOLETE

UNCLASSIFIED

1 SECURITY CLASSIFICATION OF THIS PAGE *(When Data Entered)*

163 050

transverse electromagnetic (TEM) horn antenna, which permits illumination of the test antenna with a single short pulse of energy. Special balanced configurations of the TEM horn have been developed to provide optimum radiation characteristics without the need for a conducting ground plane. A wire-grid model was developed for field testing and transportable applications. Measured transient responses of several antennas are presented. Data processing techniques for obtaining the impulse response from measured data are presented along with a comparison of predicted and measured response to a simulator.

CONTENTS

FIGURES

FIGURES (Cont'd)

1. INTRODUCTION

In recent years considerable interest has developed in the effect of transient electromagnetic signals on communication systems. Of particular concern is the disruption or damage caused to sensitive electronic components by a high-level transient voltage or current. Since the character of the disruption depends on the shape of the transient waveform, an important part of any failure analysis is an estimate of the voltages or currents coupled into the system from the electromagnetic signal. In uhf and vhf communication systems the antenna provides a major coupling path into the system for a nuclear electromagnetic pulse (EMP). It is, therefore, important to develop methods for predicting an antenna's response to EMP transient signals.

Analytical techniques have been shown to be useful for many simple antennas, but complicated antenna structures often have anomalies which are overlooked in the analytical model. Experimental techniques utilizing simulators have been developed and used to test systems at low levels and at threat levels. These techniques provide much useful information but the simulator facilities are usually large and expensive to build, operate and maintain. It is, therefore, advantageous to develop techniques which permit economical evaluation of an antenna's coupling to an EMP. Since communication antennas are generally linear devices, low-level testing is appropriate.

The Harry Diamond Laboratories (HDL) has recently been engaged in the development of a simple, low-cost, easily implemented technique to obtain the time-domain impulse response of uhf and vhf antennas. The objective is to provide research, development, test and evaluation (RDT&E) laboratories with a reliable means of evaluating EMP coupling to antennas.

There are two experimental time-domain methods for assessing the EMP vulnerability of antennas. One method is to illuminate the test antenna with a transient waveform that approximates the EMP waveform and observe the induced voltage or current. This method yields the desired result directly but is not well suited to testing of communication antennas because it is difficult to synthesize the variety of waveforms that may excite the antenna in an operating configuration. The second method is to illuminate the test antenna with a wide-bandwidth signal, usually a short pulse, and observe the induced voltage or current. The voltage or current and the incident field are then deconvolved to obtain the transfer function of the antenna. (Since communication antennas are linear devices, this operation is valid.) If the incident field is a very short pulse, the induced voltage is approximately the impulse response of the antenna and the deconvolution can be replaced by a simple normalization. The advantage of this method over the first is

that the response to any waveform can be easily computed once the transfer function is known for the desired angle of incidence and polarization.

The transverse electromagnetic (TEM) horn method for antenna transient measurements is described in section 2 of this report. The characteristics of the TEM horn radiator and the implementation of the test method are described in detail, including sources of error. Methods for processing the measured data to obtain accurate estimates of antenna transfer functions are discussed in section 3.

2. TEM HORN METHOD OF TESTING

The first step in the development of a short-pulse transient-measurement facility is selecting a means of illuminating the test antenna. Three methods of illuminating the test antenna with short pulses were considered: (1) parallel plate waveguide, (2) dipole or bicone radiator, and (3) TEM horn radiator. The parallel plate waveguide method was rejected because of the large size of the structure and the difficulties of properly terminating the waveguide. Also, such a structure is cumbersome, is expensive to construct and does not permit testing in the presence of a finitely conducting ground. Dipole and biconic radiators are often used for EMP simulators. They can radiate short pulses of electromagnetic energy that effectively illuminate the test antenna. However, reflection of the exciting current from the ends of the dipole or bicone limits the time window over which the test antenna's response may be observed.

The TEM horn radiator is an excellent alternative to dipoles and bicones for antenna transient measurements. The TEM horn, which is similar to an open-sided pyramidal horn, is a very wide-bandwidth antenna that transmits a single short pulse followed by only low-level signals. Therefore, the response of the test antenna can be observed for a very long time with minimum distortion of the impulse response. Furthermore, the TEM horn is much smaller than a dipole or bicone capable of radiating comparable bandwidth signals.

The use of the TEM horn for antenna transient measurements is depicted in figure 1. The test antenna is illuminated by a short pulse of energy that is radiated from the TEM horn when it is excited by the fast rise-time pulse. The induced voltage is measured by an appropriate receiver (e.g., a sampling oscilloscope) and recorded on an x-y recorder.

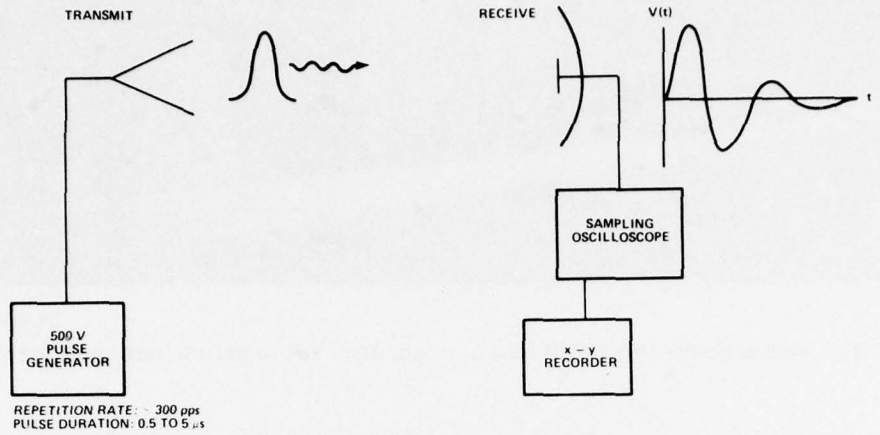

Figure 1. Antenna transient measurements by using a TEM horn radiator.

2.1 Characteristics of TEM Horn

Since the TEM horn is a key element of the measurement, its characteristics are discussed. Susman and Lamensdorf[1] have reported their results on transient antenna measurements using an unbalanced TEM horn over a ground screen. Balanced TEM horns using one and two coaxial transmission line feeds have been designed, built and tested. A typical TEM horn radiator using the two coaxial line feed is shown in figure 2. The two methods of feeding the antenna are shown in figure 3. The two coaxial line feed provides a better balanced transition that results in much less current flowing on the exterior of the feed lines and, therefore, less unwanted radiation and conduction coupling from them than does the one coaxial line feed. Both methods can be readily implemented using commercially available pulse switches, but the two feed line approach requires the pulse created by closing the switch to travel through transmission lines before reaching the radiator. The dispersion of these lines causes a slight broadening of the radiated pulse, which is not significant for EMP frequencies but may be for other applications. In the receive mode, the two coaxial line antenna requires a receiver capable of providing the algebraic difference of the two signals.

The radiation characteristics of the TEM horn can be qualitatively studied by considering the radiation from accelerating charges[2] at the leading edge of an exciting current step. Figure 4 depicts the

---

[1] *L. Susman and D. Lamensdorf, Picosecond Pulse Antenna Techniques, Rome Air Development Center Technical Report RADC-TR-71-64 (May 1971).* AD 884 646

[2] *M. Handelsman, Time Domain Impulse Antenna Study, Rome Air Development Center Technical Report RADC-TR-72-105 (May 1972).*

AD-744 837

0048-76

Figure 2. One-meter-long TEM horn used for laboratory experiments.

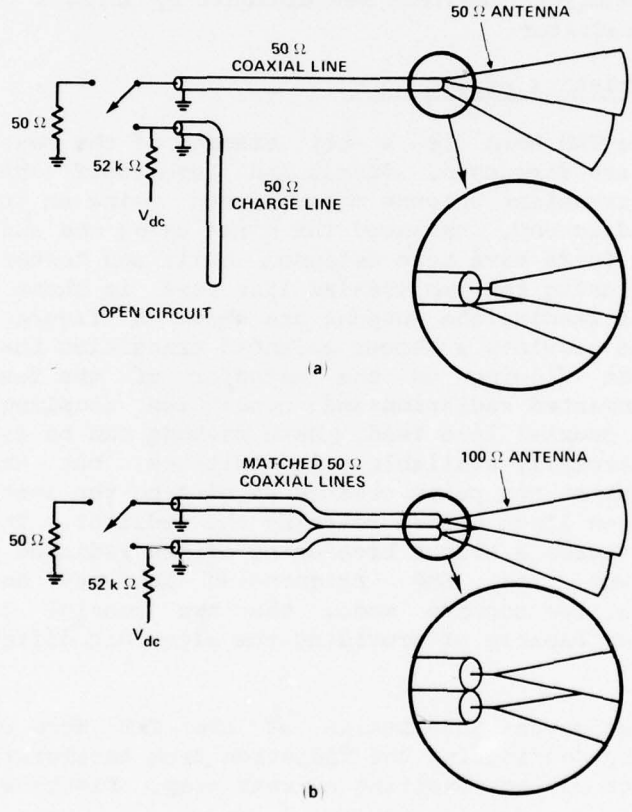

Figure 3. Two methods for feeding the TEM horn: (a) single-feed-line method and (b) two-feed-line method.

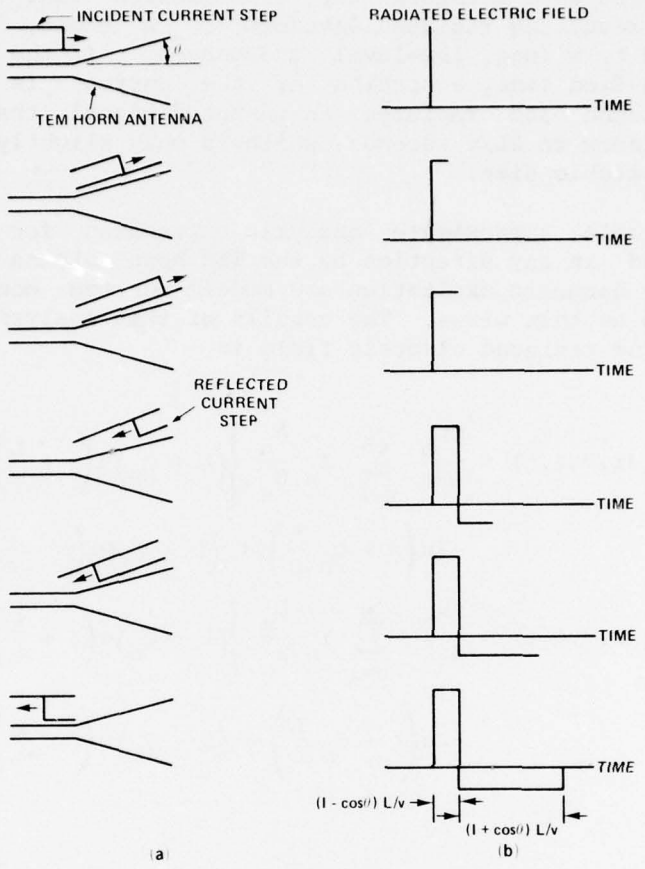

Figure 4. Radiation from TEM horn: (a) current flowing on antenna and (b) radiated field.

situation at several instances in time. The current traveling on the antenna is depicted on the left side and the radiated field is depicted on the right. Since the TEM horn has a small flare angle, radiation from the bend at the feed point is small and is ignored in this analysis. The current wave traveling out length L of the antenna with velocity v radiates strongly in the forward direction. The energy radiated during the L/v seconds that the current wave is traveling toward the observer arrives in the far field during only $(1 - \cos\theta)L/v$ seconds where θ is the angle between the conductor carrying the current and the direction of observation. After being reflected from the aperture, the current is traveling away from the observer and does not radiate as strongly in the observer's direction. Furthermore, the energy radiated during L/v seconds arrives in the far field during $(1 + \cos\theta)L/v$ seconds. If the antenna is matched to the feed line, the

returning current wave reenters the transmission line and radiation ceases. The resulting radiated waveform is a short, high-amplitude pulse followed by a long, low-level undershoot. If the antenna is not matched to the feed line, a portion of the current is reflected back onto the antenna and radiates an unwanted signal that limits the observation window to 2L/v seconds, which is only slightly better than a dipole of comparable size.

A simple, approximate analytic expression for the electric field radiated in any direction by the TEM horn antenna can be derived by considering harmonic excitation and modelling the conducting sheets of the antenna as thin wires. The details of this analysis are given in appendix A. The radiated electric field is

$$E_\theta(r,\theta,\phi,t) = \frac{c\mu_o}{4\pi r} \sum_{n=1}^{N} I_n \frac{A_n}{B_n} \left\{ (1 + C_n)u\left(\tau + \frac{L}{c}\right) - 2u\left(\tau + C_n \frac{L}{c}\right) + (1 - C_n)u\left(\tau - \frac{L}{c}\right) \right\},$$

$$E_\phi(r,\theta,\phi,t) = \frac{c\mu_o}{4\pi r} \sum_{n=1}^{N} I_n \frac{D_n}{B_n} \left\{ (1 + C_n)u\left(\tau + \frac{L}{c}\right) - 2u\left(\tau + C_n \frac{L}{c}\right) + (1 - C_n)u\left(\tau - \frac{L}{c}\right) \right\}, \quad (1)$$

where

c = velocity of light,

μ_o = permeability of free space,

I_n = amplitude of current wave on nth wire,

$A_n = \sin(\theta - \theta_n) + \cos\theta \sin\theta_n \left[1 - \cos(\phi - \phi_n)\right]$,

$B_n = \left[\sin\theta \sin\theta_n \cos(\phi - \phi_n) + \cos\theta \cos\theta_n\right]^2 - 1$,

$C_n = \sin\theta \sin\theta_n \cos(\phi - \phi_n) + \cos\theta \cos\theta_n$,

$D_n = \sin\theta_n \sin(\phi - \phi_n)$,

θ_n, ϕ_n = spherical coordinate directions of nth wire,

$u(t)$ = unit step function,

$\tau = t - r/c$,

L = length of wires.

The z axis is oriented along the center line of the antenna. These expressions are easily obtained from the usual frequency domain expression for radiation from a traveling current wave (see, for example, Walter[3]).

The Fourier transform of the ideal waveform corresponding to a 1-m-long TEM horn is shown in figure 5 along with the spectrum of the three-impulse signal radiated by a bicone of 1-m half-length. These spectra assume that zero rise time signals excite the antennas. The finite rise time of the actual signals modifies the high-frequency portion of the radiated waveform as can be seen in the data of figure 6. The 0-deg waveform has the basic shape depicted in figure 4. The positive pulse is broadened and rounded (fig. 6) because of the finite rise time of the current step. The ripples in the undershoot are the result of ripples on the incident current step. Off boresight, the radiation changes in the manner predicted by equation (1). The increase in amplitude of the positive pulse at 30 deg is due to improved radiation at angles farther off the direction of the current flow. The waveform radiated to the rear--180 deg--is approximately the mirror image of the forward waveform but is lower in amplitude and more spread out due to the radiation of much of the high-frequency energy in the forward direction and to some recapture of backward traveling energy.

There are two important characteristics that must be considered when the TEM horn is used as a transient radiator. First, the antenna feed line must be well matched and balanced to prevent unwanted reflections and radiation. The two coaxial line method minimizes this problem and should always be used when accurate results are required. Second, since the TEM horn differentiates the exciting current waveform, the energy content of the radiated pulse is small compared to the energy content of the step function excitation. This is not a significant disadvantage for low-level testing because the "step function" is actually a fast rise-time pulse that lasts only long enough to observe the complete transient response of the antenna (usually less than 1 μs). Therefore, the duty factor is low (<0.01 percent) and the average power requirements are easily met by ordinary laboratory equipment.

---

[3] *C. H. Walter, Traveling Wave Antennas, McGraw-Hill Book Co., New York (1965).*

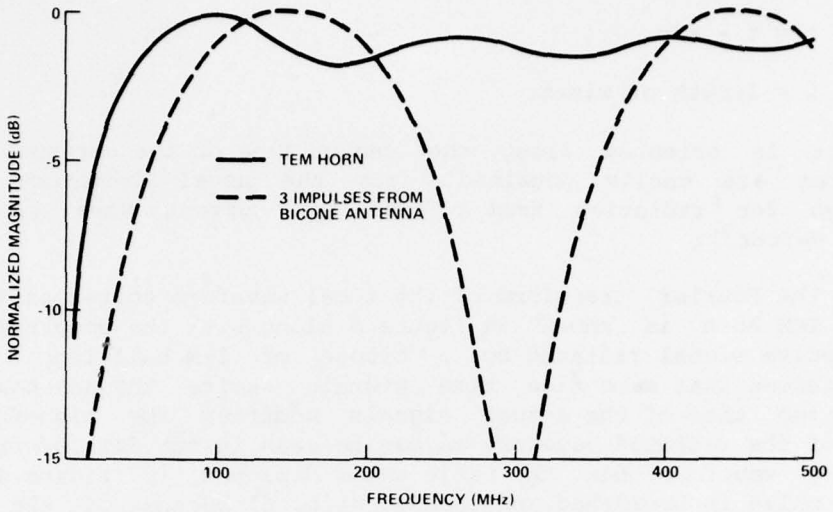

Figure 5. Normalized amplitude spectra of ideal pulses radiated by 1-m-long, 50-ohm TEM horn and biconic antenna of 1-m half-length.

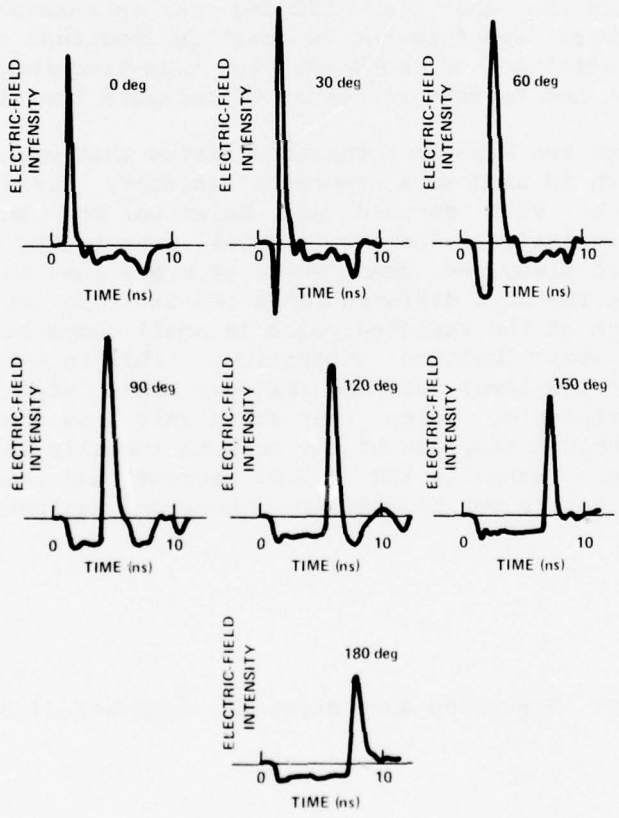

Figure 6. Actual signal radiated by TEM horn at several angles in E-plane.

2.2 Antenna Transient Measurements

The implementation of the TEM horn method of antenna testing is straightforward but care must be taken to insure that maximum accuracy is obtained. The TEM horn radiator is used to illuminate the test antenna and the voltage delivered to the antenna's load is detected with an appropriate receiver and recorded. The receiver/recorder used to obtain the data presented here was a laboratory sampling oscilloscope and an x-y recorder (see fig. 1). The sampling oscilloscope can be used because the pulse generator, a vibrating mercury switch, provides approximately 300 pps with excellent pulse-to-pulse stability. Other possible receivers for transient antenna measurements include boxcar averagers, real-time oscilloscopes and transient data recorders. The most important requirement of the receiver/recorder is that it accurately display transient signals having bandwidths of 50:1 or greater and instantaneous dynamic ranges of 30 to 50 dB.

The ordinary laboratory equipment illustrated in figure 1 meets the minimum requirements. However, standard programmable test equipment under the control of an instrumentation computer provides much greater accuracy, bandwidth and dynamic range. Real-time or postmeasurement signal averaging techniques[4,5] are effective ways to improve transient antenna measurements. Also, computer controlling of the experiment permits efficient handling of the large quantities of data that can be produced by these measurements. Automated testing is recommended for users requiring high accuracy or for users planning extensive transient testing. The results presented in this report, however, illustrate the effectiveness of transient testing with ordinary laboratory equipment.

In addition to the precautions that should be observed in constructing and using the TEM horn radiator (see sect. 2.1), special consideration should be given to the layout of cables and test equipment. The broad bandwidth signals used in transient testing are capable of exciting many resonances within the experimental setup. Therefore, it is imperative that unwanted coupling to the equipment and cables be minimized. Signal and power cables that are not part of the test antenna and that are exposed to the illuminating field should be shielded as much as possible and oriented orthogonally to the electric field. In some cases, ferrite beads placed around cables will help to reduce unwanted coupling. Direct exposure of the receiver/recorder to the electric field should be avoided or minimized. Direct connections

---

[4] *F. J. Deadrick, E. K. Miller, and H. G. Hudson, The LLL Transient-Electromagnetics-Measurement Facility, University of California Lawrence Livermore Laboratory Report UCRL-51933 (October 1975).*

[5] *C. L. Bennett, Impulse Response Measurements and Results, Proceedings of National Conference on Electromagnetic Scattering (June 1976).*

between the transmit and receive antennas, such as trigger signal cables and ac power lines, should always be checked to insure that they do not provide coupling paths.

A useful variation of the test procedure described above is easily obtained from the time-domain reciprocity theorem,[6,7] which states that the receive transfer function, $h_R(t)$, of an antenna is related to the transmit transfer function, $h_T(t)$, by

$$h_R(t) \propto \int_0^t h_T(\tau)\, d\tau \ . \qquad (2)$$

This means that the electric field radiated by the test antenna when it is excited by a *step function* is proportional to the receive transfer function. In some cases, it may be more convenient to interchange the transmit and receive antennas in figure 1 and use reciprocity to obtain $h_R(t)$.

2.3 Transportability and Field Implementations

The TEM horn antenna shown in figure 2 is an excellent transient radiator for laboratory testing. However, if very-low-frequency excitations are required, a longer antenna must be used (see fig. 5) and out-of-doors testing will be required. A large TEM horn constructed of conducting sheets as shown in figure 2 would be heavy and would experience considerable forces from winds. To overcome these problems, a TEM horn using thin wire conductors was designed. This antenna is lightweight and experiences little wind loading. Furthermore, the antenna is constructed to permit easy assembly and disassembly for transportable field testing.

A prototype of the 1-m feed section for a wire TEM horn radiator is shown in figure 7. The inset shows the construction of the two coaxial line feed. The semirigid coaxial lines pass through a brass tube that provides structural support and the outer conductors of the coaxial lines are soldered to the end cap to insure that currents flow from one transmission line to the other with minimum reflection. Operational models will be permanently encapsulated in strong, lightweight fiberglass instead of Plexiglas. The TEM horn radiator is assembled by connecting lengths of flexible wire to each of the elements

---

[6] *H. J. Schmitt, Transients in Cylindrical Antenna, IEE Monograph 377 E (April 1960), 292.*

[7] *B. R. Mayo, Generalized Linear Radar Analysis, Microwave Journal, 4 (1961), 79.*

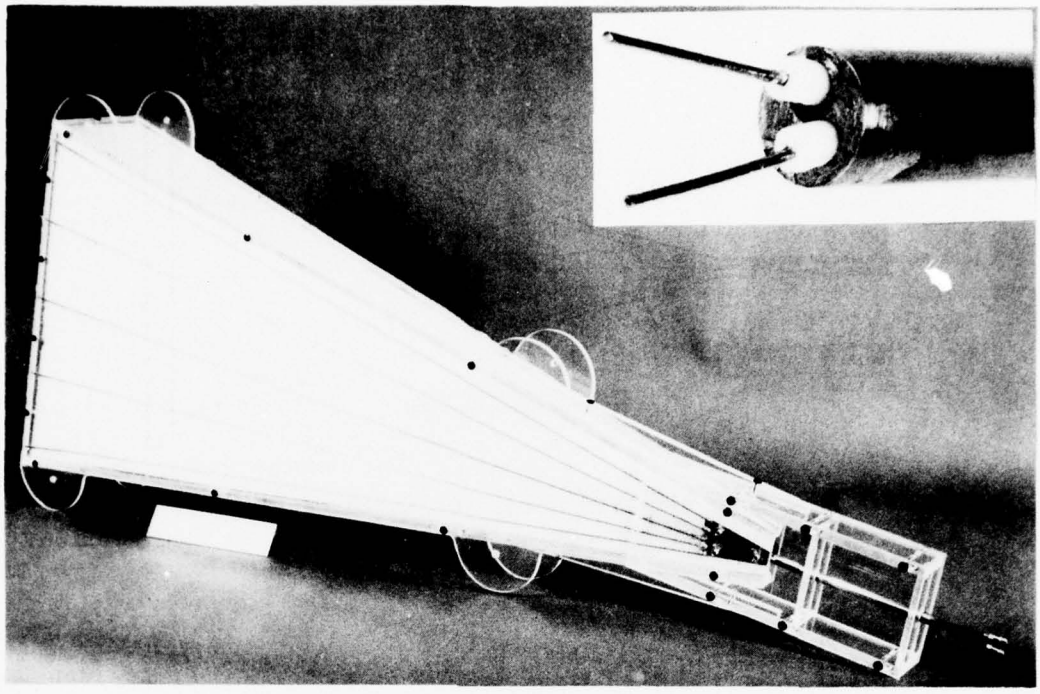

477-76

Figure 7. Prototype of 1-m-long feed section for wire TEM horn radiator. Inset shows feed lines that are attached to antenna.

protruding from the feed section and anchoring them at the aperture as shown in figure 8. Intermediate supports can be used as required, but very long antennas are needed only for extremely low frequencies.

Because of its relatively small size, the TEM horn can be easily rotated to provide either horizontal or vertical polarization. Also, the TEM horn is a self-contained radiator that does not require termination to the ground. Therefore, it can be readily elevated to provide illumination from above the test antenna.

Key design criteria for the wire TEM horn radiator are essentially the same as for the solid conductor antenna. The impedance should be matched at the feed point and remain relatively constant along the length of antenna. The impedance of the wire TEM horn feed section is shown in figure 9. By keeping wire separations less than about one half of the pulse length, TEM mode propagation is maintained and the impedance remains relatively constant despite increasing wire separation as the antenna flares.

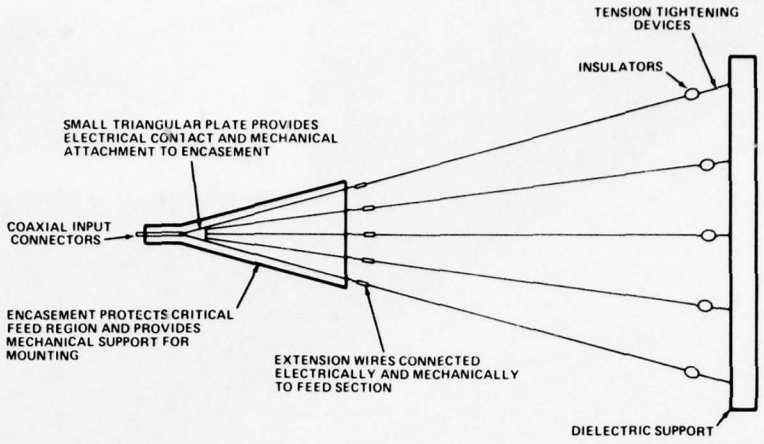

Figure 8. Very long wire TEM horns for field testing are easily assembled by connecting lengths of wire to feed section.

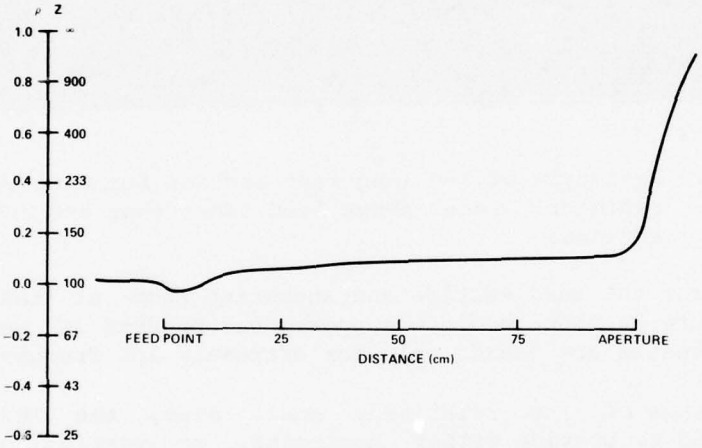

Figure 9. Time-domain reflectometer plot of impedance of prototype wire feed section shown in figure 7.

2.4 Typical Results

Many antennas have been tested by using the TEM horn method. Some of the tests were performed inside the HDL anechoic chamber and some were performed out-of-doors at HDL's Woodbridge Research Facility. Figure 6 shows the electric field radiated by a 1-m-long TEM horn. Figure 10 shows the electric field radiated in the 0-deg boresight direction by a 2-m-long TEM horn. The negative undershoot following the main pulse lasts for approximately 12 ns (twice as long as for the 1-m antenna) as is predicted by equation (1). The positive radiation that follows the negative undershoot is due, in part, to reflection of currents from the single coaxial feed line used for this TEM horn.

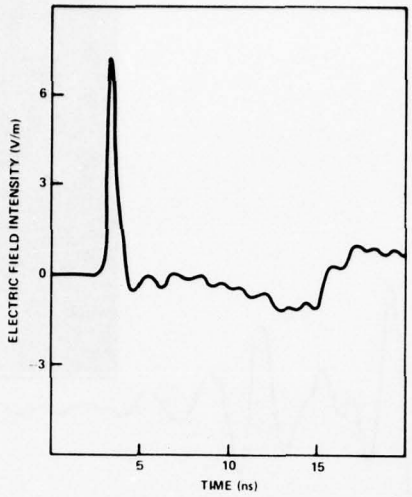

Figure 10. Radiated electric field of 2-m-long TEM horn.

A standard gain dipole was tested by using the TEM horn method and the results are shown in figure 11. Another antenna that has been tested is the Army's AS-1852 (fig. 12). The voltage delivered to a 50-ohm load for various angles of incidence in the E-plane is shown in figure 13.

A yagi antenna with three stagger-tuned driven elements also was tested. The transient response of the antenna (fig. 14) appears to be a modulated, damped sinusoid. The fundamental frequency of 280 MHz and the modulation frequency of 30 MHz are clearly discernible. The effective height versus frequency of the antenna (obtained from transient data) closely resembles the spectrum of an amplitude modulated wave. The three elements of the yagi are tuned to approximately 250, 280 and 310 MHz.

The data of figures 11, 13 and 14 were obtained by using the 1-m TEM horn shown in figure 2 inside the anechoic chamber. The data that follow were obtained out-of-doors at the Woodbridge Research Facility by using the 1-m wire TEM horn shown in figure 7 or the 4-m wire TEM horn formed by attaching extra lengths of wire to the 1-m antenna as discussed in the previous section.

The electric field radiated by the 1-m-long wire TEM horn is shown in figure 15. The antenna used as the field probe is shown in figure 16. The voltage received by this antenna is an excellent reproduction of the electric field up to the time when the currents reflected from the shorting disk return to the feed point (approximately 18 ns for this antenna). The response of the yagi antenna in figure 14

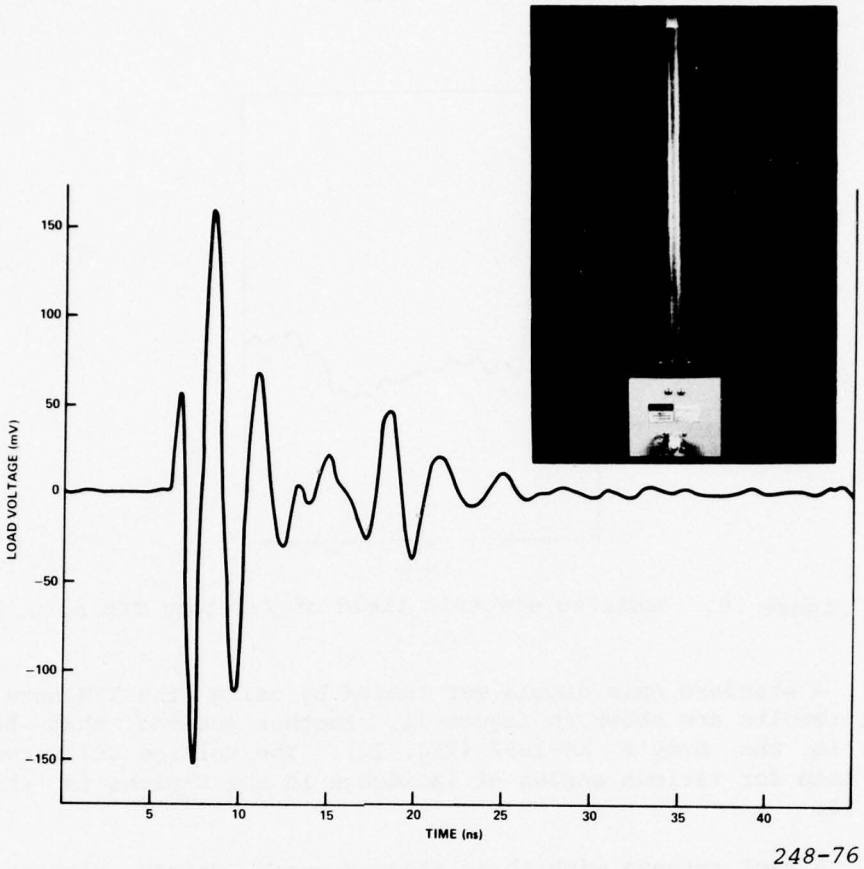

Figure 11. Transient measurements of standard gain dipole.

to this electric field is shown in figure 17. The electric field that illuminates the yagi includes the direct and the ground reflected signals. Therefore, the voltage in figure 17 is the antenna's response to the total ground-interacted field. For some applications, it is very useful to be able to measure directly this ground-interacted transfer function. For other applications, the free space transfer function is required. Then the incident field and the measured response must be deconvolved by using one of the techniques discussed in section 3.

The electric field observed at a distance of 19 m from the 4-m wire TEM horn is shown in figure 18. The trailing edge of the pulse remains positive for an extended period because the ground-reflected pulse arrives at the observation point about 3 ns after the direct signal and cancels the negative undershoot. (The electric field is vertically polarized for this measurement.)

The response of the 1-m TEM horn in figure 2 to this electric field is shown in figure 19. Several important features are evident in this response. The received voltage is approximately proportional to the incident electric field. This proportionality is what is expected since the receive transfer function of the TEM horn is identical to the field radiated when the TEM horn is excited by a step function (see

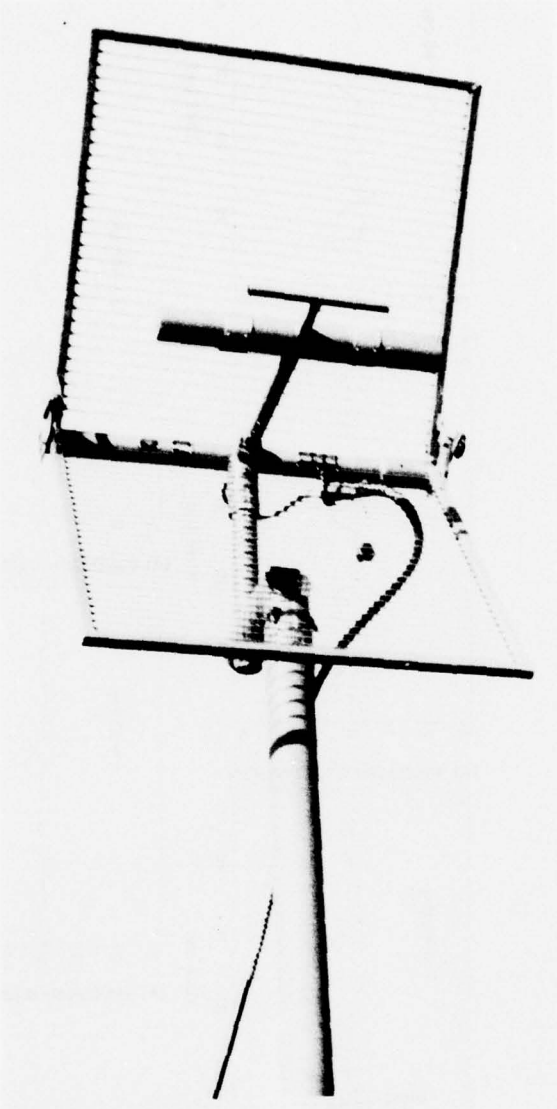

23-75

Figure 12. The AS-1852 antenna with band I element.

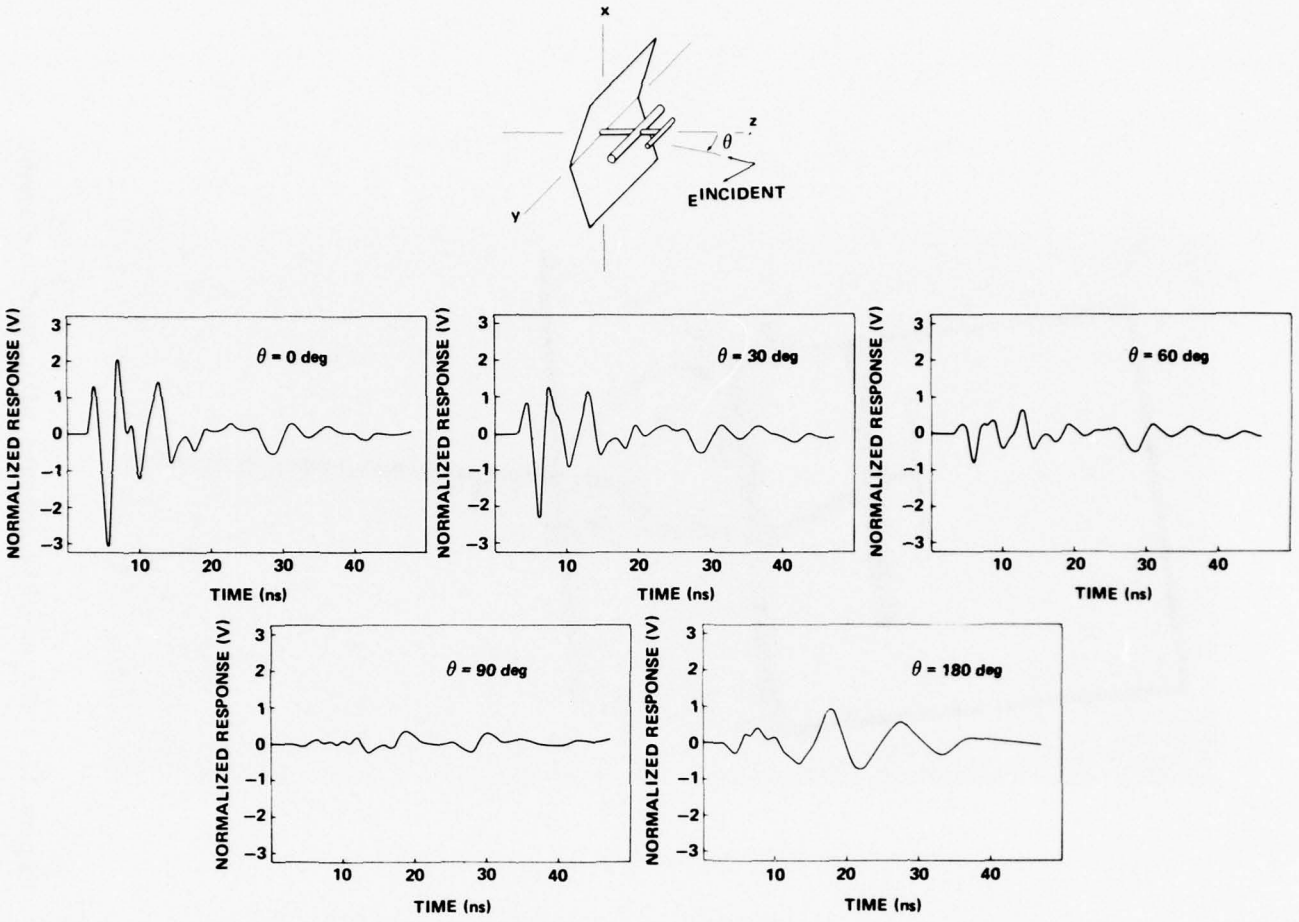

Figure 13. Response of AS-1852 antenna to pulse from TEM horn. Normalized responses show received signal for various angles of incidence in E-plane.

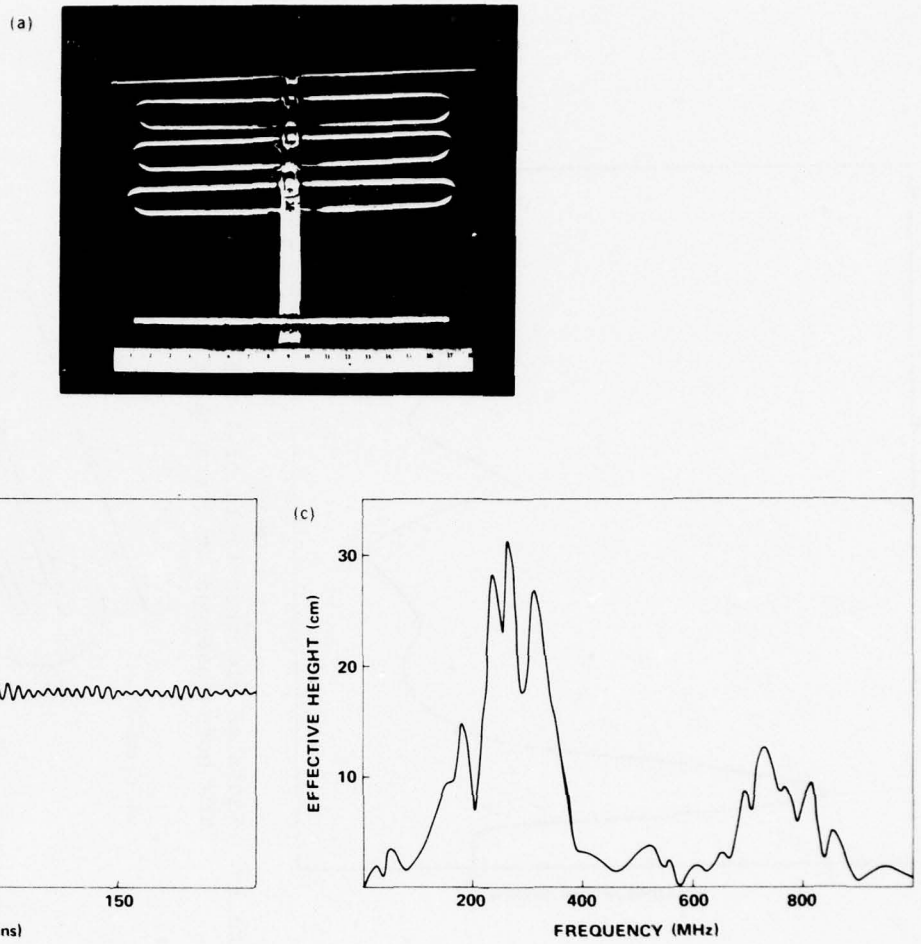

Figure 14. Transient response of yagi antenna: (a) yagi antenna, (b) transient response and (c) effective height.

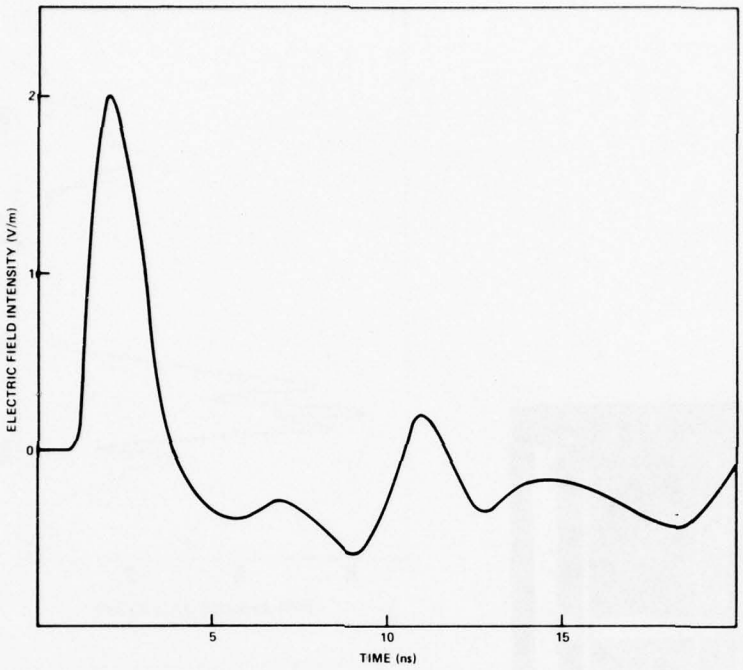

Figure 15. Radiated electric field of 1-m-long prototype wire TEM horn observed at distance of 11 m.

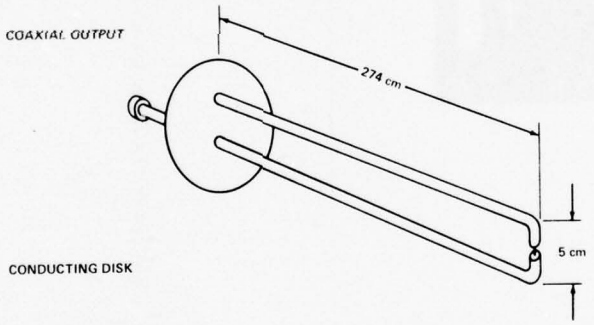

Figure 16. Antenna used to observe early time behavior of electric field.

fig. 4). This follows from the time-domain reciprocity theorem.[6,7] After the initial pulse, the received voltage differs substantially from the incident electric field. The deviations can be traced to the characteristics of the TEM horn antenna. Some of the negative undershoot is due to the negative undershoot characteristic of the

---

[6] *H. J. Schmitt, Transients in Cylindrical Antenna, IEE Monograph 377 E (April 1960), 292.*

[7] *B. R. Mayo, Generalized Linear Radar Analysis, Microwave Journal, 4 (1961), 79.*

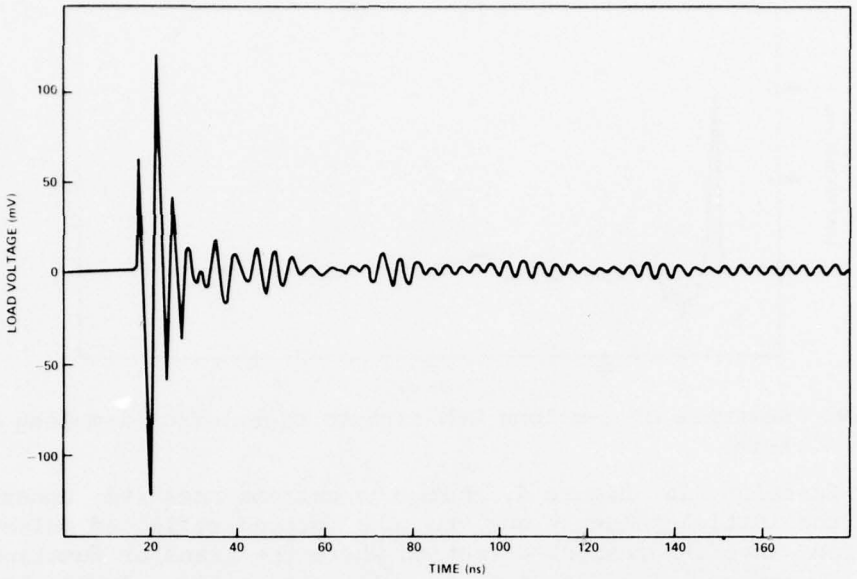

Figure 17. Response of yagi antenna to total, ground-interacted electric field.

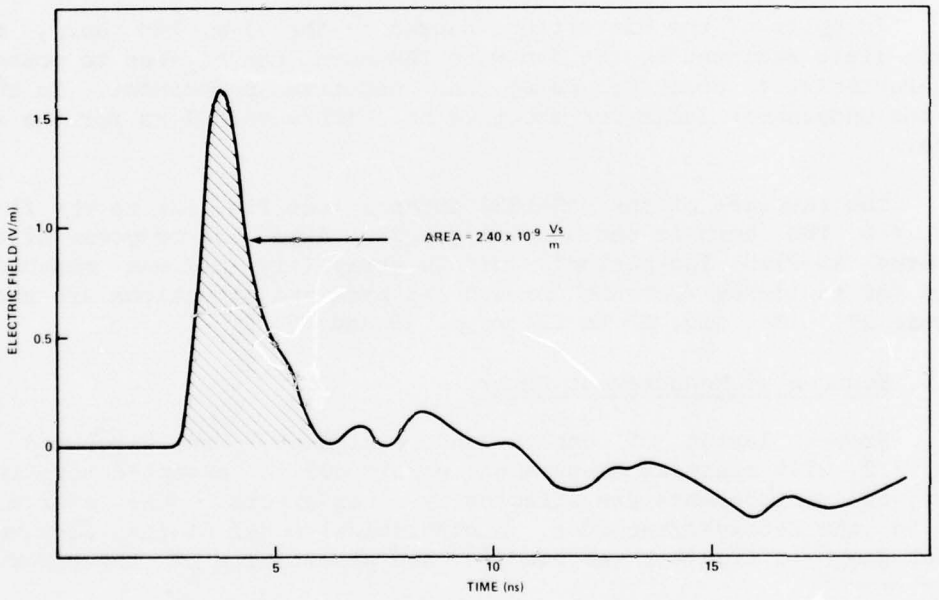

Figure 18. Radiated electric field of 4-m-long wire TEM horn antenna observed at distance of 19 m.

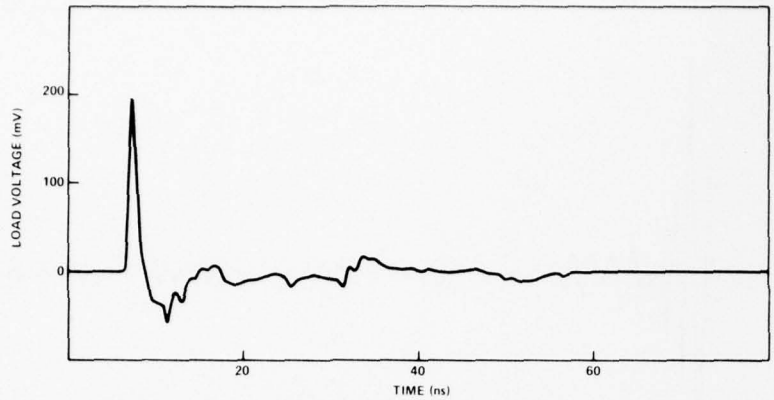

Figure 19. Response of 1-m-long TEM horn to signal from 4-m-long TEM horn.

transfer function in figure 4, but the extreme negative undershoot following the initial pulse is due to the ground reflected pulse that arrives from an off-boresight direction where the transfer function has an initial negative spike (see fig. 6). Another portion of the received voltage that is characteristic of the 1-m antenna is the small reflection or ringing caused by a small mismatch at the feed point. This ringing has a period of about 6 ns.

In spite of the distortions caused by the 1-m TEM horn, the electric field radiated by the 4-m wire TEM horn can be seen to possess the characteristic positive pulse and negative undershoot. In this case, the undershoot lasts for about 24 ns. ($2L/v = 26.7$ ns for the 4-m antenna.)

The response of the AS-1852 antenna (see fig. 12) to the field of the 4-m TEM horn is shown in figure 20. Also, the response of the U.S. Army AS-2169 log-periodic dipole array (fig. 21) was measured. Results for incidence from the forward and backward directions are shown in figure 22. (See fig. 20 to 22 on pp. 25 and 26.)

2.5 Sources of Measurement Error

Proper layout of cables and equipment, as discussed in section 2.2, will minimize measurement errors due to unwanted coupling. However, the measurements are affected by other errors. One source of error is the receiver/recorder. A statistical model of the receiver/recorder shown in figure 1 was studied[8] and an estimate of the error in

[8] *Daniel H. Schaubert, Arthur R. Sindoris, and Frederick G. Farrar, A Measurement Technique for Determining the Time-Domain Voltage Response of uhf Antennas to EMP Excitation, Harry Diamond Laboratories TR-1778 (August 1976).*

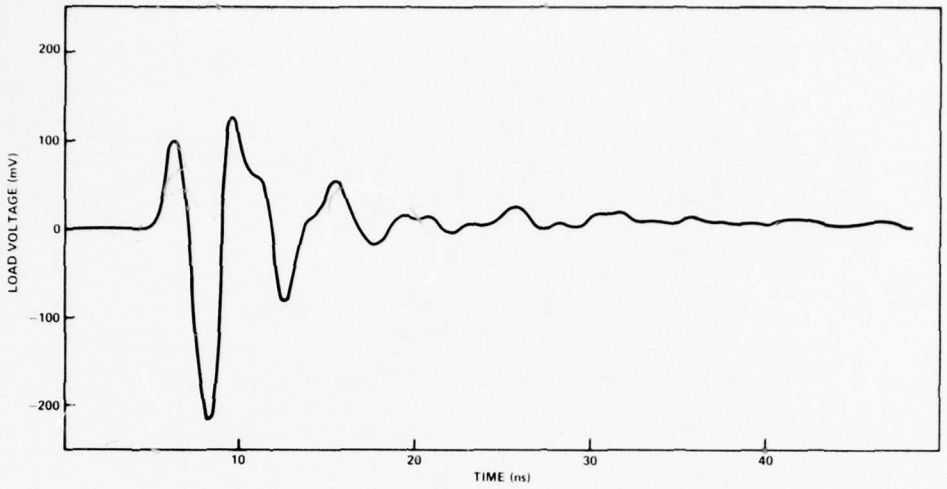

Figure 20. Response of AS-1852 antenna to signal from 4-m-long TEM horn.

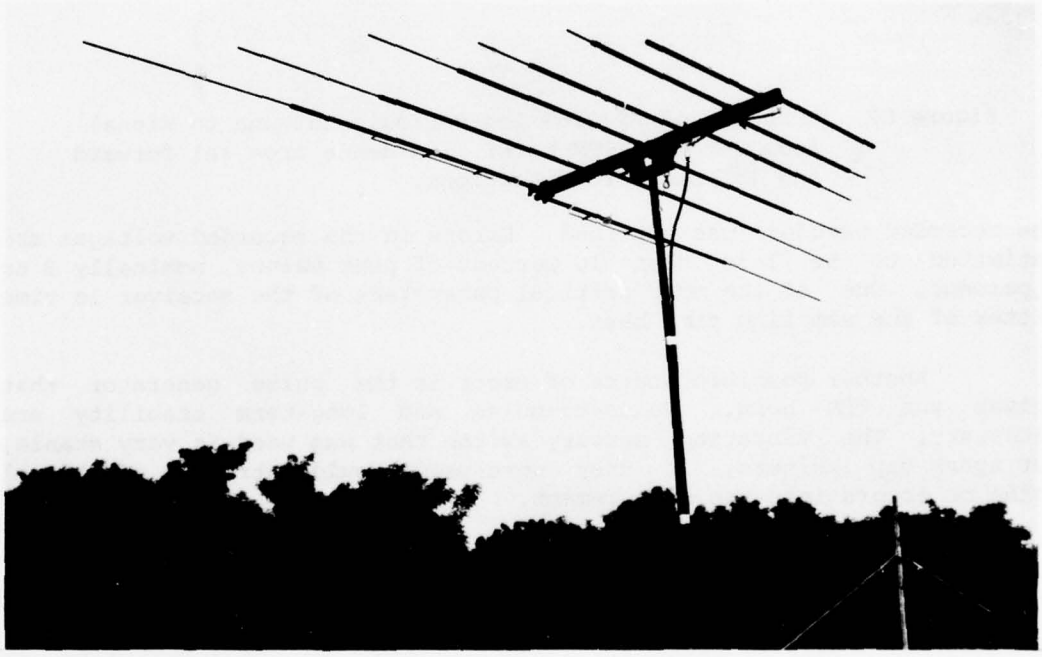

425-75

Figure 21. The AS-2169 log-periodic dipole array; operating frequency: 30 to 76 MHz.

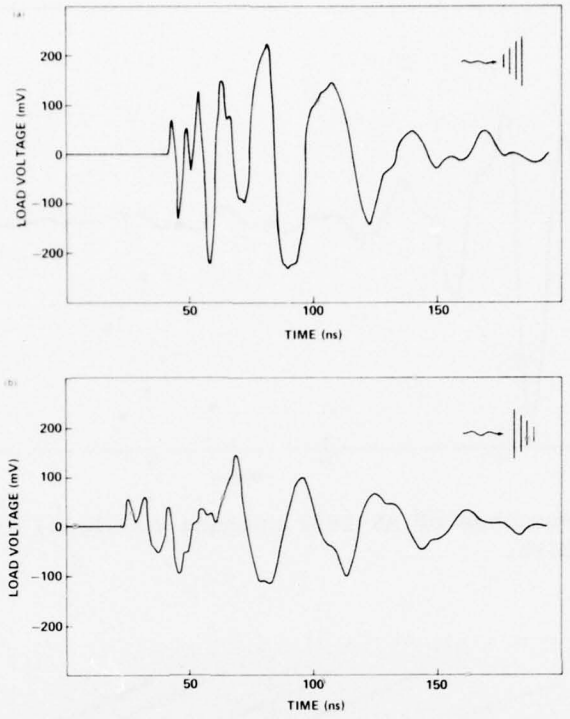

Figure 22. Response of AS-2169 log-periodic antenna to signal from 4-m-long TEM horn: incidence from (a) forward and (b) backward directions.

the recorded waveform was obtained. Errors in the recorded voltages are estimated to be less than 10 percent of peak values, nominally 3 to 5 percent. One of the most critical parameters of the receiver is time jitter of the sampling time base.

Another possible source of error is the pulse generator that drives the TEM horn. Pulse-to-pulse and long-term stability are necessary. The vibrating mercury switch that was used is very stable, but spark gap pulsers, if they were used, could introduce additional noise or errors into the measurement.

To use the transfer function to compute EMP response it is necessary to assume that the test antenna is illuminated by a plane wave. This means that the separation between the TEM horn and the test antenna must satisfy the far-field criterion for all frequencies of interest. To do so, the maximum path length difference between points on the transmit and receive antennas must be small compared to the width of the radiated pulse.

Secondary illumination of the test antenna by reflected signals also can contribute errors to the measured response. Unwanted reflections (as distinguished from the intentional ground reflection that defines the ground-interacted transfer function) that arrive after the initial pulse cause distortions in the late-time response of the antenna. These distortions cannot always be removed by deconvolution because they do not arrive from the same direction as the initial pulse. (Recall that $h_R(t)$ is, in general, dependent upon the angle of incidence.)

Some of the data presented in this report were taken inside the HDL anechoic chamber. The chamber walls attenuate reflected signals more than 30 dB at 200 MHz and above, but less than 10 dB below 50 MHz. It was found that useful data on EMP coupling could be obtained in the anechoic chamber for antennas that operate above 200 MHz and for scale models of lower-frequency antennas. The advantages of testing in the anechoic chamber include excellent signal-to-noise ratios and the ability to isolate the receiver/recorder by placing it outside the chamber. The absorption of the chamber walls permits determination of the free space transfer functions for high frequencies (greater than 200 MHz).

3. DATA PROCESSING

The response voltages measured by using the TEM horn method represent an approximation to the receive transfer function of the test antenna. The response, $v(t)$, is an approximate transfer function because the incident electric field is an approximate impulse, that is,

$$v(t) = \int_0^t e(t - \tau) h_R(\tau)\, d\tau \,, \tag{3}$$

where $e(t)$ = incident electric field $\simeq \delta(t)$.

An improved estimate of the transfer function can be obtained by deconvolving the measured voltage and the incident field. The improvement that can be achieved is limited to correcting for the nonideal impulse waveform that radiates directly from the TEM horn to the test antenna. The effects of reflections arriving from various angles of incidence cannot be corrected by deconvolution because $h_R(t)$ depends also on the angle of incidence. Three methods of processing the measured data to obtain $h_R(t)$ are discussed below. Another method, direct numerical solution of the time-domain convolution integral equation, was tried and found to be unsatisfactory because of the poor conditioning of the convolution equation. The kernel function, $e(t)$, and the forcing function, $v(t)$, are measured data and contain noise that causes the solution to be unstable.

3.1 Method I: Normalization

The simplest form of data processing does not attempt to correct the measured waveform to account for the incident waveform. Instead, the measured voltage is simply normalized to account for the amount of energy in e(t). That is, $h_R(t)$ is evaluated from

$$h_R(t) = Cv(t) \ , \tag{4}$$

where

$$C = \frac{1}{\text{area of the incident pulse}} \ .$$

This normalization is consistent with the usual requirement that the unit delta function have an area of one. Figure 18 demonstrates the computation of the area of the pulse.

Figures 23 and 24 show transfer functions obtained by normalizing the response voltages measured at the Woodbridge Research Facility by using the 4-m wire TEM horn radiator. The area of the incident pulse was 2.40×10^{-9} Vs/m.

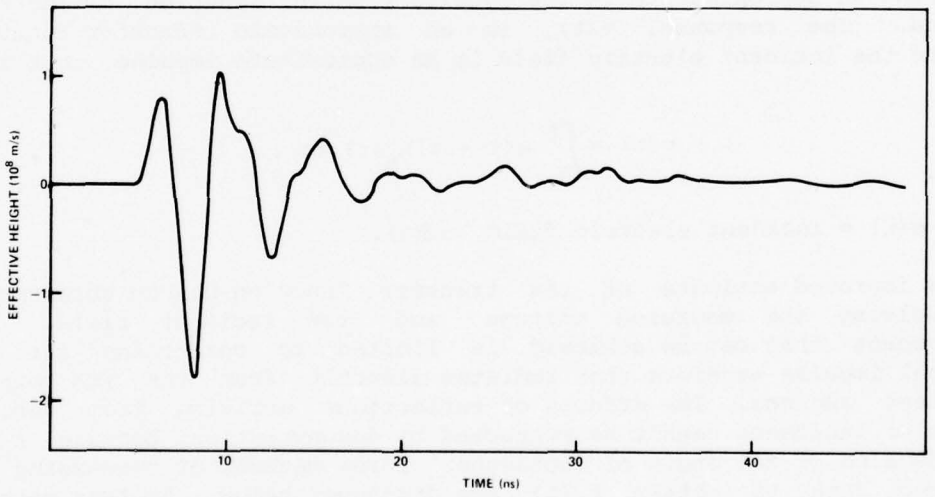

Figure 23. Time-domain transfer function of AS-1852 antenna obtained via normalization method.

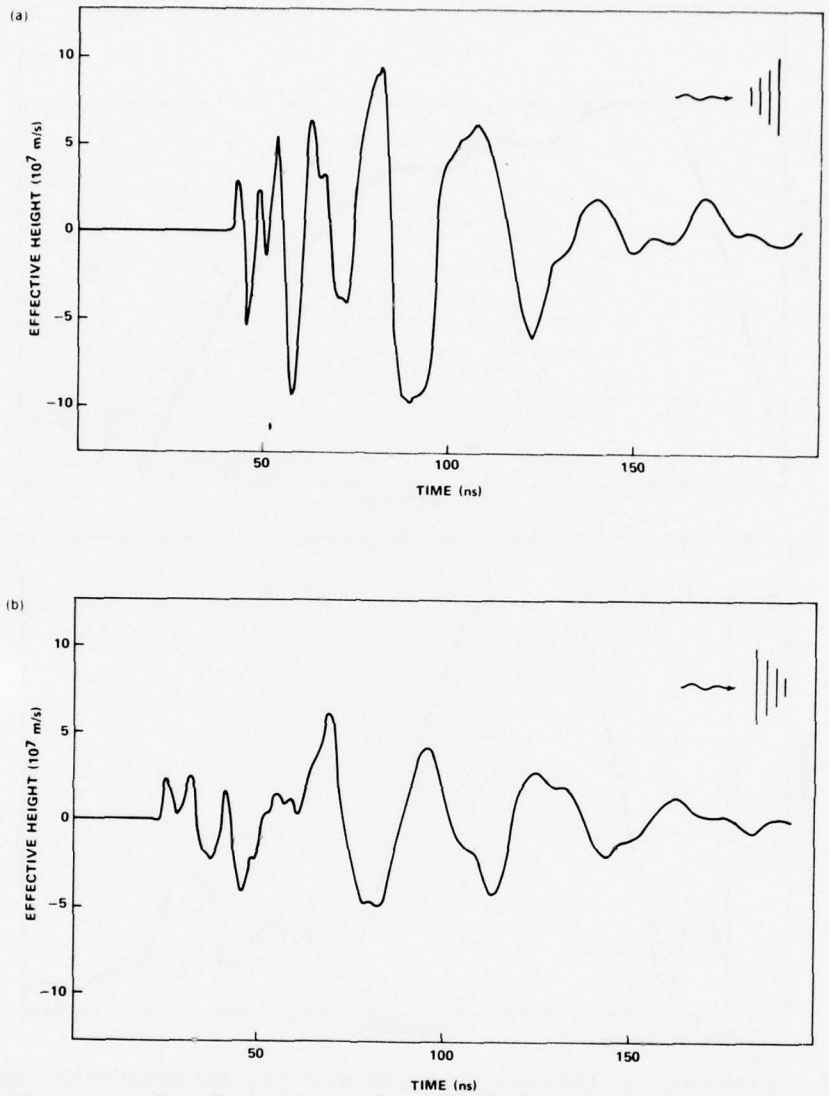

Figure 24. Transfer functions of AS-2169 log-periodic antenna obtained via normalization method: incidence from (a) forward and (b) backward directions.

3.2 Method II: Fast Fourier Transform

Equation (3) can be numerically deconvolved by dividing the Fourier transform of v(t) by the transform of e(t). The fast Fourier transform (FFT) algorithm makes this operation practical, but measurement and numerical noise must be filtered out in order to obtain useful results. A rectangular bandpass filter applied to the spectrum of v(t) has yielded good results. The cutoff frequencies of the filter are established by using the following criteria (see also fig. 25):

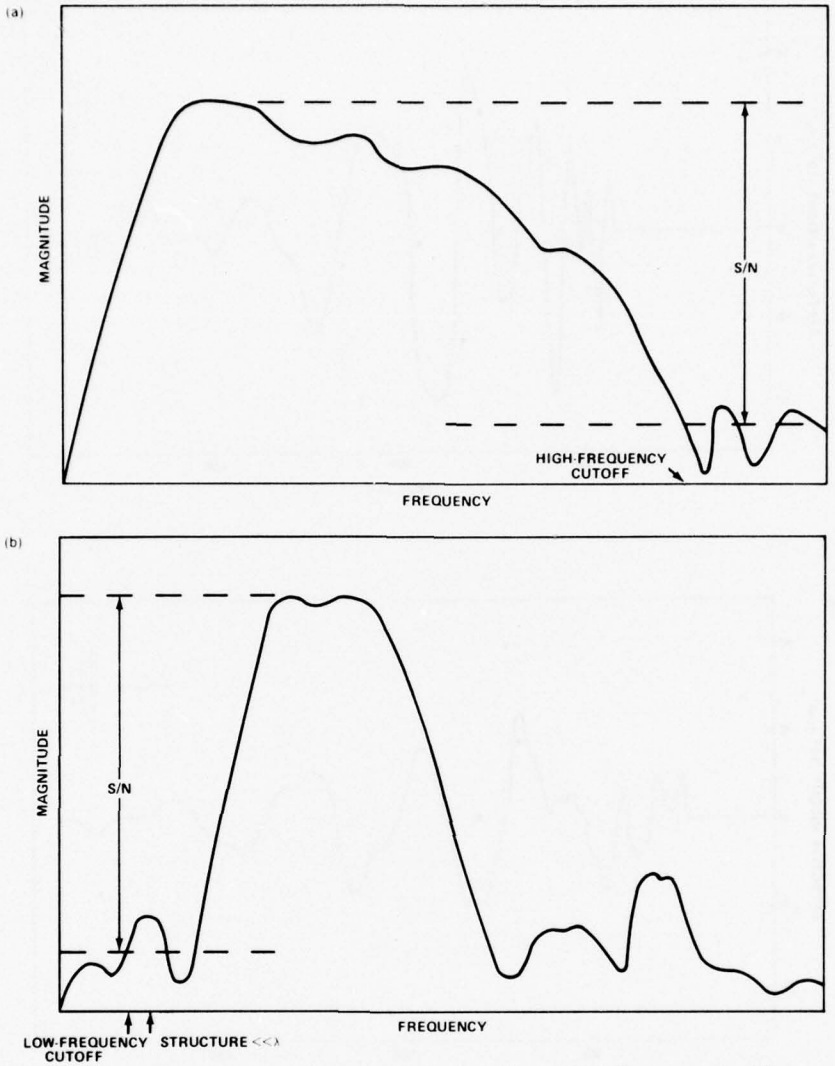

Figure 25. Bandwidth selection criteria for FFT deconvolution method: (a) spectrum of incident field and (b) spectrum of response.

a. The filter passband includes all of the test antenna's designed operating band.

b. The high-frequency cutoff eliminates all points of the incident field spectrum that are more than the signal-to-noise ratio below the peak components.

c. The low-frequency cutoff eliminates all points of the response voltage spectrum that are more than the signal-to-noise ratio below the peak components and that have wavelengths much greater than the largest dimension of the test structure.

The corrected transfer functions in figures 26 and 27 were obtained by using the FFT method. Since the illuminating pulse is very broad band, these transfer functions are not dramatically different from those calculated by using simple normalization. The transfer functions in figure 27 were convolved with the electric field radiated by an EMP simulator and compared to a previously measured response.[9] The results (fig. 28) show very good agreement. Peak amplitudes compare to within 10 percent and all significant details of the response are predicted. The accuracy of the TEM horn method of testing and its low cost and ease of implementation make it a useful technique for determining critical coupling paths and highly vulnerable configurations prior to high-level system tests. Also, the method can be used to verify computer codes and data from previous tests. The relatively small size of the TEM horn allows it to be transported and setup in configurations not possible with other transient radiators.

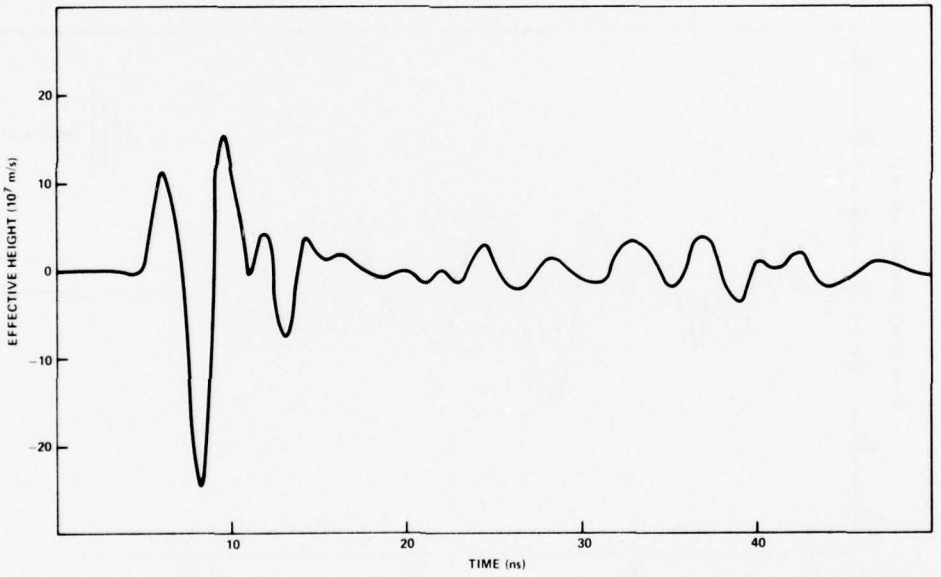

Figure 26. Transfer function of AS-1852 obtained via FFT method.

[9]*Werner J. Stark, Transient Response of a Log-Periodic Antenna Based on Broad-Band Continuous-Wave Measurements, Harry Diamond Laboratories TR-1792 (April 1977).*

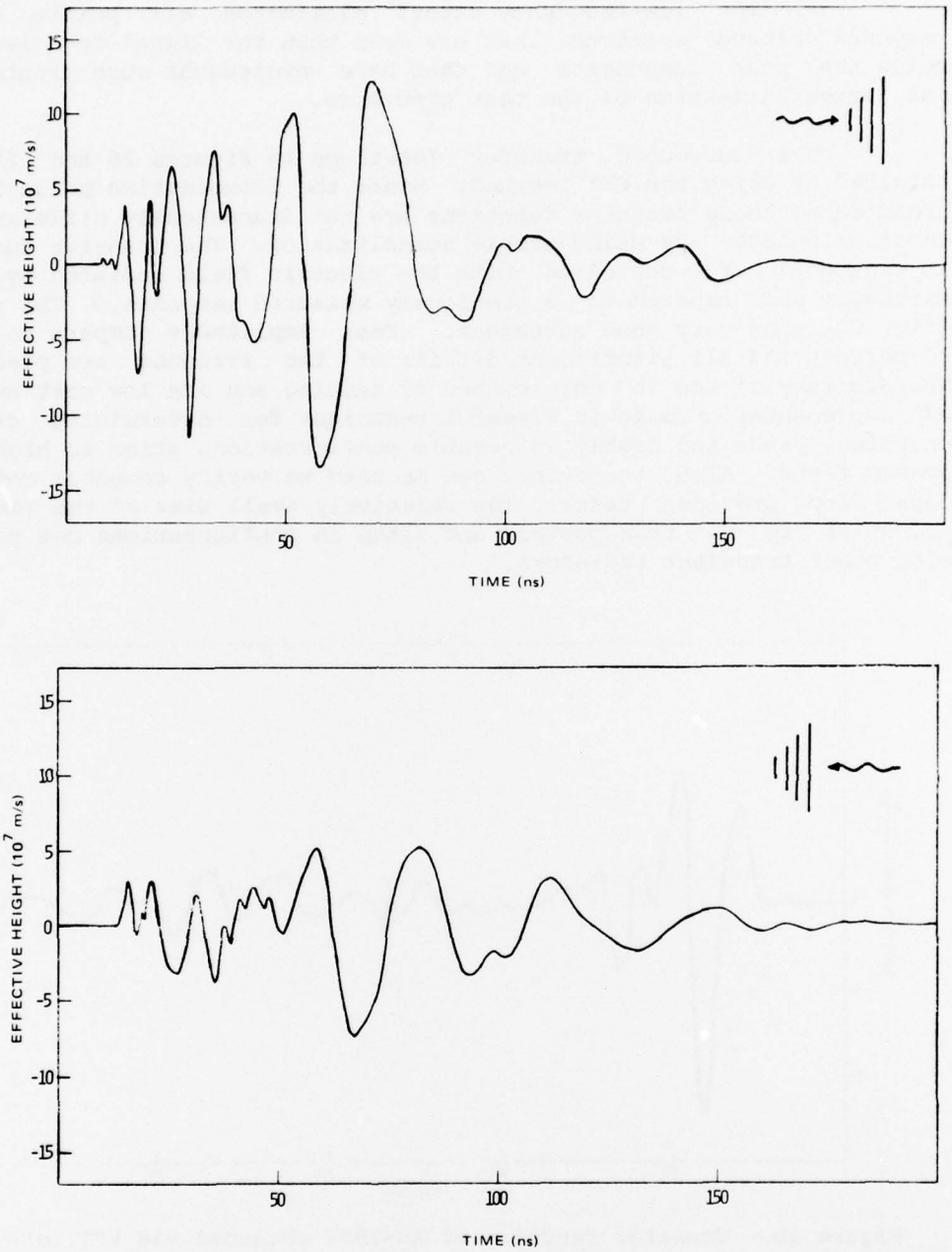

Figure 27. Transfer functions of AS-2169 obtained via FFT method.

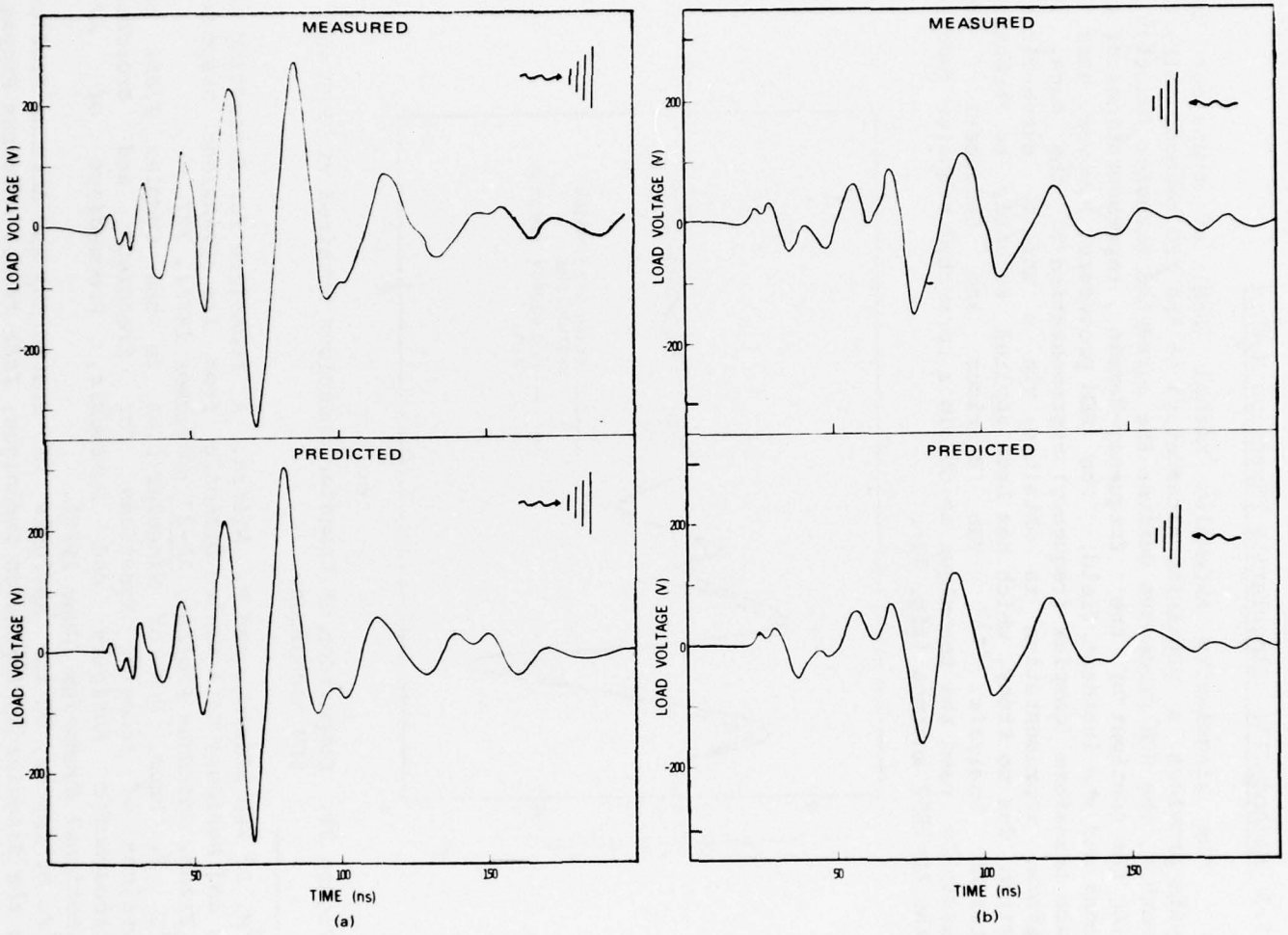

Figure 28. Measured and predicted responses of the AS-2169 log-periodic antenna to EMP simulator: incidence from (a) forward and (b) backward directions.

3.3 Method III: Singularity Expansion Method

The singularity expansion method (SEM) of transient data analysis provides a promising alternative to the FFT method. Like the FFT method, the SEM procedure derives the corrected transfer function by forming the quotient of the frequency-domain representations of the response and the incident field. The SEM procedure, however, uses the Laplace transform (complex frequency) representation of the data. The transform representation is obtained via a unique curve-fitting algorithm due to Prony, which has been applied recently to transient scattering analysis.[10-12] Van Blaricum and Schaubert[13] have successfully used the technique to obtain a corrected transfer function for the AS-1852 antenna (fig. 29).

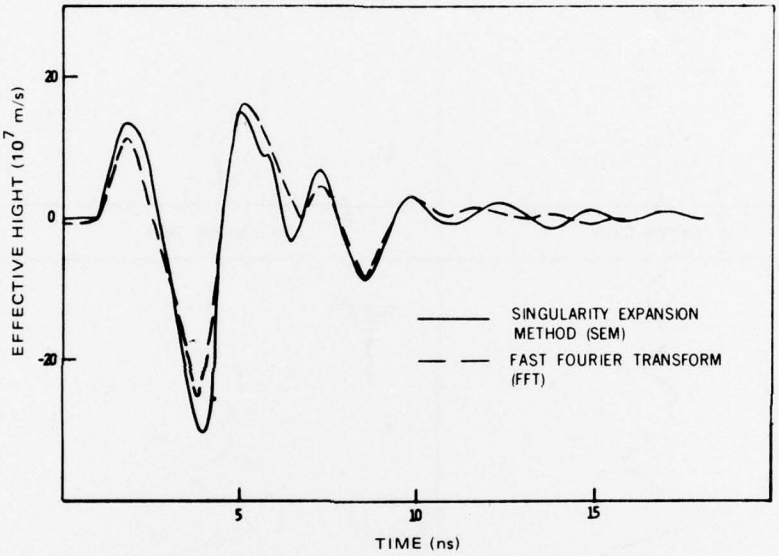

Figure 29. Comparison of transfer functions obtained via FFT and SEM techniques.

---

[10] *M. L. Van Blaricum and R. Mittra, A Technique for Extracting the Poles and Residues of a System Directly from Its Transient Response, IEEE Trans. Antennas Propag., AP-23 (November 1975), 777.*

[11] *C. E. Baum, Use of Singularities in the Complex Plane and Eigenvalues of Integral Equations for Transient and Broadband Electromagnetic Analysis and Synthesis, Proceedings of AP-S International Symposium (June 1975).*

[12] *F. M. Tesche, On the Analysis of Scattering and Antenna Problems Using the Singularity Expansion Technique, IEEE Trans. Antennas Propag., AP-21 (January 1973), 53.*

[13] *M. L. Van Blaricum and D. H. Schaubert, An Experimental Transient Transfer Function via Prony's Method, Proceedings of USNC/URSI Meeting (October 1976).*

The SEM procedure consists of approximating a transient waveform, f(t), by a finite sum of complex exponentials; that is,

$$f(t) \approx \sum_{n=1}^{N} A_n e^{s_n t} . \tag{5}$$

Prony's algorithm allows one to compute the complex pole frequencies, s_n, and complex residues, A_n, from the sampled function values, $f(m\Delta t)$. Completeness of the representation in equation (5) for antenna problems has not been proven, but numerous analytical and experimental results have verified the engineering usefulness of the expression. The Laplace transform, F(s), is obtained immediately from equation (5):

$$F(s) \approx \sum_{n=1}^{N} \frac{A_n}{s - s_n} . \tag{6}$$

In addition to possible computational savings, the SEM representations are useful because the waveform f(t) is completely defined by a relatively small set of complex numbers (the coefficients A_n and poles s_n). Also, equation (6) can be rewritten as

$$F(s) = \frac{P(s)}{Q(s)} , \tag{7}$$

where P and Q are polynomials. In this form, the theorems of lumped element circuit analysis are directly applicable to the transfer function. If P and Q satisfy the realizability criteria, an equivalent lumped-element circuit model of the antenna can be obtained. Another advantage of equation (5) is that it can be analytically convolved with typical EMP waveforms to obtain a closed form expression for the response signal.

4. CONCLUSIONS

A transient testing procedure that provides reliable estimates of coupling to communication antennas has been demonstrated. The procedure, which uses a TEM horn to transmit a very short pulse of energy, is easy and inexpensive to implement and provides a direct measurement of the impulse response of the antenna. Because the pulse is radiated and not contained by a guiding structure, direct measurement of ground-interacted transfer functions is possible. On the other hand,

testing in a minimum reflection environment provides the free space transfer function. The TEM horn was chosen as the transmit antenna because it is much smaller than a biconic or dipole antenna capable of radiating the very wide bandwidth pulses that are needed for EMP coupling measurements. Since the TEM horn does not require a termination to ground, it can be easily moved and elevated to provide illumination from various angles of incidence. Furthermore, wire grid TEM radiators have been built and shown to be excellent transient radiators for field and transportable testing requirements. The TEM horn is, however, useful only for low-level testing since it requires step function (long duration, high-energy pulse) excitation.

Posttest processing of the data can be performed in a variety of ways. The simplest way requires only a scaling of the received voltage to determine the approximate transfer function. More sophisticated processing, however, can yield more accurate estimates of the transfer function. Furthermore, if computer-controlled test equipment is available, a large number of data points can be averaged to further improve the accuracy of the results.

Antennas of practical interest, including two Army communication antennas, have been tested by using the TEM horn method. The measured responses were processed to obtain the antennas' transfer functions, which were used to predict the responses to a pulse from an EMP simulator. Comparison with measured simulator data indicated that accuracies of 5 to 10 percent can be achieved with ordinary laboratory test equipment.

LITERATURE CITED

(1) L. Susman and D. Lamensdorf, Picosecond Pulse Antenna Techniques, Rome Air Development Center Technical Report RADC-TR-71-64 (May 1971).

(2) M. Handelsman, Time Domain Impulse Antenna Study, Rome Air Development Center Technical Report RADC-TR-72-105 (May 1972).

(3) C. H. Walter, Traveling Wave Antennas, McGraw-Hill Book Co., New York (1965).

(4) F. J. Deadrick, E. K. Miller, and H. G. Hudson, The LLL Transient-Electromagnetics-Measurement Facility, University of California Lawrence Livermore Laboratory Report UCRL-51933 (October 1975).

(5) C. L. Bennett, Impulse Response Measurements and Results, Proceedings of National Conference on Electromagnetic Scattering (June 1976).

(6) H. J. Schmitt, Transients in Cylindrical Antenna, IEE Monograph 377 E (April 1960), 292.

(7) B. R. Mayo, Generalized Linear Radar Analysis, Microwave Journal, 4 (1961), 79.

(8) Daniel H. Schaubert, Arthur R. Sindoris, and Frederick G. Farrar, A Measurement Technique for Determining the Time-Domain Voltage Response of uhf Antennas to EMP Excitation, Harry Diamond Laboratories TR-1778 (August 1976).

(9) Werner J. Stark, Transient Response of a Log-Periodic Antenna Based on Broad-Band Continuous-Wave Measurements, Harry Diamond Laboratories TR-1792 (April 1977).

(10) M. L. Van Blaricum and R. Mittra, A Technique for Extracting the Poles and Residues of a System Directly from Its Transient Response, IEEE Trans. Antennas Propag., AP-23 (November 1975), 777.

(11) C. E. Baum, Use of Singularities in the Complex Plane and Eigenvalues of Integral Equations for Transient and Broadband Electromagnetic Analysis and Synthesis, Proceedings of AP-S International Symposium (June 1975).

(12) F. M. Tesche, On the Analysis of Scattering and Antenna Problems Using the Singularity Expansion Technique, IEEE Trans. Antennas Propag., AP-21 (January 1973), 53.

(13) M. L. Van Blaricum and D. H. Schaubert, An Experimental Transient Transfer Function via Prony's Method, Proceedings of USNC/URSI Meeting (October 1976).

APPENDIX A.--RADIATION FROM THE TEM HORN

A simple, approximate analytic expression for the field radiated by the transverse electromagnetic (TEM) horn can be derived when the conducting surfaces of the horn are modelled by wires as shown in figure A-1. The feed point is located at the origin, the z axis is along the boresight direction of the antenna and the wire elements are of length L. The impedance of the antenna is assumed to be matched to the source so that no reflections occur at the feed point. At the aperture, the current reflection coefficient is R. Assuming harmonic excitation and uniform current flow (a valid assumption since the impedance of the TEM horn is constant along its length), the current on the nth wire is

$$i_n(s) = I_n e^{j\omega t}\left[e^{-j\beta(s-L)} + Re^{j\beta(s-L)}\right] , \qquad (A\text{-}1)$$

where

s = position variable along wire,

I_n = magnitude of nth current,

β = propagation constant along wire.

For a perfect open circuit $R = -1$ and $i_n(s) = 0$ at $s = L$.

By using the standard technique of computing the vector potential $\bar{A}$, the fields radiated by i_n are readily determined. Figure A-2 shows the angles γ, θ_o, ϕ_o, θ_n and ϕ_n relating the point of observation and the nth wire.

$$\bar{A}_n = \hat{s}_n \frac{\mu_o}{4\pi}\int_o^L i_n(s) \frac{e^{-jkr}}{r}\, ds , \qquad (A\text{-}2)$$

where

$\hat{s}_n$ = unit vector in direction of nth wire,

μ_o = permeability of free space,

$k = \omega/c$ = propagation constant of free space,

r = distance between source and observation points.

APPENDIX A

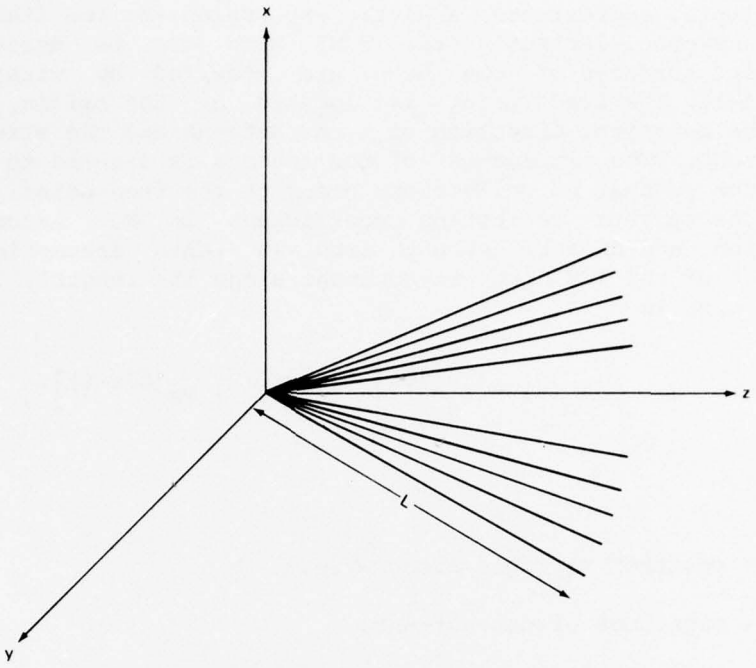

Figure A-1. Wire model used to compute approximate radiated fields of TEM horn.

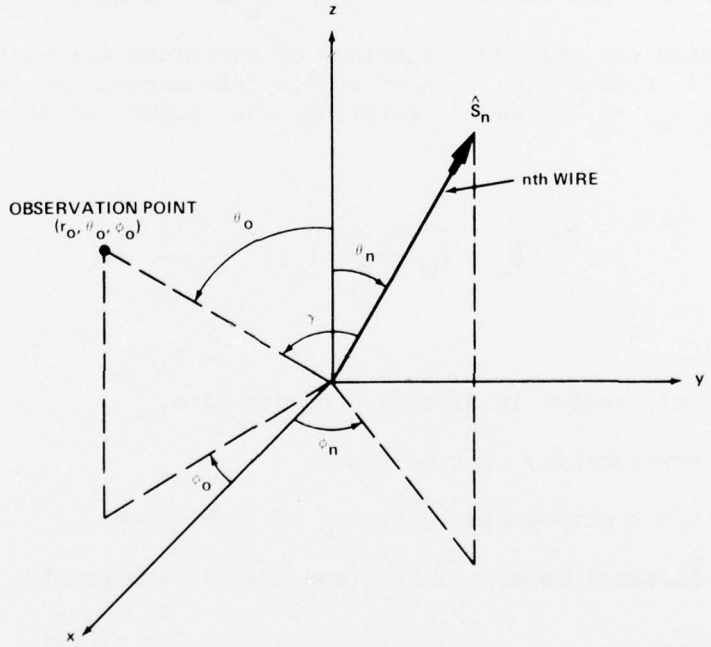

Figure A-2. Coordinate variables for expressing radiation of nth wire.

When r is large, the far-field approximation reduces equation (A-2) to

$$\begin{aligned}\bar{A}_n &= -\hat{s}_n \frac{\mu_o e^{-jkr_o}}{4\pi r_o} \int_o^L i_n(s) e^{jk \cos \gamma s}\, ds \\ &= -\hat{s}_n \frac{\mu_o I_n e^{-j(kr_o - \omega t)}}{4\pi r_o} \int_o^L \left[e^{j\beta L} e^{j(k \cos \gamma - \beta)s} \right. \\ &\quad \left. + R e^{-j\beta L} e^{j(k \cos \gamma + \beta)s} \right] ds \\ &= -\hat{s}_n \frac{\mu_o I_n L e^{-j(kr_o - \omega t)}}{4\pi r_o} \left(e^{jA} \frac{\sin B}{B} + R e^{jB} \frac{\sin A}{A} \right), \end{aligned} \tag{A-3}$$

where

$$A = (k \cos \gamma + \beta)\frac{L}{2} ,$$

$$B = (k \cos \gamma - \beta)\frac{L}{2} .$$

This vector potential can be used to determine the far-zone fields ($\bar{H} = \nabla \times \bar{A}$) of the nth wire when it is excited by a single frequency, ω. The fields radiated by the TEM horn when it is excited by a transient signal are obtained by summing (integrating) the weighted response over all frequencies and adding together the fields radiated by each wire in the model. For example, the radiated fields due to a step excitation are found by multiplying equation (A-3) by $1/\omega$ (the spectrum of a step function), integrating and adding the contributions of each wire. Expressing γ in terms of θ_o, ϕ_o, θ_n and ϕ_n and setting $R = -1$ and $\beta = k$, the step response of a typical TEM horn is obtained:

$$\begin{aligned} E_\theta(r,\theta,\phi,t) = \frac{c\mu_o}{4\pi r} \sum_{n=1}^{N} I_n \frac{A_n}{B_n} \Bigg\{ &\left(1 + C_n\right) u\left(\tau + \frac{L}{c}\right) \\ &-2u\left(\tau + C_n \frac{L}{c}\right) + \left(1 - C_n\right) u\left(\tau - \frac{L}{c}\right) \Bigg\} , \end{aligned} \tag{A-4}$$

$$\begin{aligned} E_\phi(r,\tau,\phi,t) = \frac{c\mu_o}{4\pi r} \sum_{n=1}^{N} I_n \frac{D_n}{B_n} \Bigg\{ &\left(1 + C_n\right) u\left(\tau + \frac{L}{c}\right) \\ &-2u\left(\tau + C_n \frac{L}{c}\right) + \left(1 - C_n\right) u\left(\tau - \frac{L}{c}\right) \Bigg\} , \end{aligned} \tag{A-5}$$

where

c = velocity of light,

μ_o = permeability of free space,

I_n = amplitude of current wave on nth wire,

$A_n = \sin\left(\theta - \theta_n\right) + \cos\theta \sin\theta_n \left[1 - \cos\left(\phi - \phi_n\right)\right]$,

$B_n = \left[\sin\theta \sin\theta_n \cos\left(\phi - \phi_n\right) + \cos\theta \cos\theta_n\right]^2 - 1$,

$C_n = \sin\theta \sin\theta_n \cos\left(\phi - \phi_n\right) + \cos\theta \cos\theta_n$,

$D_n = \sin\theta_n \sin\left(\phi - \phi_n\right)$,

θ_n, ϕ_n = spherical coordinate directions of nth wire,

$u(t)$ = unit step function,

$\tau = t - r/c$,

L = length of wires.

These expressions can be used to determine the radiated fields in any direction. Furthermore, replacing the step functions with delta functions yields the impulse response, which can be used to compute the fields for any excitation.

DISTRIBUTION

DEFENSE DOCUMENTATION CENTER
CAMERON STATION, BUILDING 5
ALEXANDRIA, VA 22314
ATTN DDC-TCA (12 COPIES)

COMMANDER
US ARMY MATERIEL DEVELOPMENT
& READINESS COMMAND
5001 EISENHOWER AVENUE
ALEXANDRIA, VA 22333
ATTN DRXAM-TL, HQ TECH LIBRARY
ATTN DRCPM-SCM-WF
ATTN DRCDE-D/COL J. F. BLEECKER
ATTN DRCDE, DIR FOR DEV & ENGR
ATTN DRCDE-DE/H. DARRACOTT
ATTN DRCMS-I/DR. R. P. UHLIG
ATTN DRCMS-I/MR. E. O'DONNEL

COMMANDER
US ARMY ARMAMENT MATERIEL
READINESS COMMAND
ROCK ISLAND ARSENAL
ROCK ISLAND, IL 61201
ATTN DRSAR-ASF, FUZE & MUNITION SPT DIV
ATTN DRSAR-PDM/J. A. BRINKMAN
ATTN DRCPM-VFF

COMMANDER
USA MISSILE & MUNITIONS CENTER & SCHOOL
REDSTONE ARSENAL, AL 35809
ATTN ATSK-CTD-F

DEFENSE ADVANCED RESEARCH
PROJECTS AGENCY
1400 WILSON BLVD
ARLINGTON, VA 22209
ATTN TECH INFORMATION OFFICE

DIRECTOR
DEFENSE COMMUNICATION ENG CENTER
1860 WIEHLE AVENUE
RESTON, VA 22090
ATTN R104, M. J. RAFFENSPERGER
ATTN R800, R. E. LYONS

DIRECTOR
DEFENSE INTELLIGENCE AGENCY
WASHINGTON, DC 20301
ATTN DI-2, WEAPONS & SYSTEMS DIV

DIRECTOR
DEFENSE NUCLEAR AGENCY
WASHINGTON, DC 20305
ATTN PETER HAAS, DEP DIR,
SCIENTIFIC TECHNOLOGY
ATTN RAEV, CPT WILSON
ATTN VLIS, LTC SHIMERDA

DEPARTMENT OF DEFENSE
DIRECTOR OF DEFENSE RESEARCH & ENGINEERING
WASHINGTON, DC 20301
ATTN DEP DIR (TACTICAL WARFARE PROGRAMS)
ATTN DEP DIR (TEST & EVALUATION)
ATTN DEFENSE SCIENCE BOARD

CHAIRMAN
JOINT CHIEFS OF STAFF
WASHINGTON, DC 20301
ATTN J-3, NUCLEAR WEAPONS BR
ATTN J-3, EXER PLANS & ANALYSIS DIV
ATTN J-5, NUCLEAR DIR NUCLEAR POLICY BR
ATTN J-5, REQUIREMENT & DEV BR
ATTN J-6, COMMUNICATIONS-ELECTRONICS

DEPARTMENT OF DEFENSE
JOINT CHIEFS OF STAFF
STUDIES ANALYSIS & GAMING AGENCY
WASHINGTON, DC 20301
ATTN TAC NUC BR
ATTN SYS SUPPORT BR

ASSISTANT SECRETARY OF DEFENSE
PROGRAM ANALYSIS AND EVALUATION
WASHINGTON, DC 20301
ATTN DEP ASST SECY (GEN PURPOSE PROG)
ATTN DEP ASST SECY (REGIONAL PROGRAMS)
ATTN DEP ASST SECY (RESOURCE ANALYSIS)

DEPARTMENT OF THE ARMY
OFFICE, SECRETARY OF THE ARMY
WASHINGTON, DC 20301
ATTN ASST SECRETARY OF THE ARMY (I&L)
ATTN DEP FOR MATERIEL ACQUISITION
ATTN ASST SECRETARY OF THE ARMY (R&D)

DEPARTMENT OF THE ARMY
ASSISTANT CHIEF OF STAFF FOR INTELLIGENCE
WASHINGTON, DC 20301
ATTN DAMI-OC/COL J. A. DODDS
ATTN DAMI-TA/COL F. M. GILBERT

US ARMY SECURITY AGENCY
ARLINGTON HALL STATION
4000 ARLINGTON BLVD
ARLINGTON, VA 22212
ATTN DEP CH OF STAFF RESEARCH
& DEVELOPMENT

DIRECTOR
WEAPONS SYSTEMS EVALUATION GROUP
OFFICE, SECRETARY OF DEFENSE
400 ARMY-NAVY DRIVE
WASHINGTON, DC 20305
ATTN DIR, LT GEN GLENN A. KENT

DEPARTMENT OF THE ARMY
DEPUTY CHIEF OF STAFF FOR OPERATIONS & PLANS
WASHINGTON, DC 20301
ATTN DAMO-RQD/COL E. W. SHARP
ATTN DAMO-SSP/COL D. K. LYON
ATTN DAMO-SSN/LTC R. E. LEARD
ATTN DAMO-SSN/LTC B. C. ROBINSON
ATTN DAMO-RQZ/COL G. A. POLLIN, JR.
ATTN DAMO-TCZ/MG T. M. RIENZI
ATTN DAMO-ZD/A. GOLUB
ATTN DAMO-RQZ/LTC L. A. WEIZEL

DEPARTMENT OF THE ARMY
CHIEF OF RESEARCH, DEVELOPMENT,
AND ACQUISITION OFFICE
WASHINGTON, DC 20301
ATTN DAMA-RAZ-A/R. J. TRAINOR
ATTN DAMA-CSM-N/LTC OGDEN
ATTN DAMA-WSA/COL W. E. CROUCH, JR.
ATTN DAMA-WSW/COL L. R. BAUMANN
ATTN DAMA-CSC/COL H. C. JELINEK
ATTN DAMA-CSM/COL H. R. BAILEY
ATTN DAMA-WSZ-A/MG D. R. KEITH
ATTN DAMA-WSM/COL J. B. OBLINGER, JR.
ATTN DAMA-PPR/COL D. E. KENNEY

COMMANDER
BALLISTIC MISSILE DEFENSE SYSTEMS
P.O. BOX 1500
HUNTSVILLE, AL 35807
ATTN BMDSC-TEN/MR. JOHN VEFNEMAN

COMMANDER
US ARMY FOREIGN SCIENCE
AND TECHNOLOGY CENTER
220 SEVENTH ST., NE
CHARLOTTESVILLE, VA 22901

DIRECTOR
US ARMY MATERIEL SYSTEMS
ANALYSES ACTIVITY
ABERDEEN PROVING GROUND, MD 21005
ATTN DRXSY-C/DON R. BARTHEL
ATTN DRXSY-T/P. REID

COMMANDER
US ARMY SATELLITE COMMUNICATIONS AGENCY
FT. MONMOUTH, NJ 07703
ATTN LTC HOSMER

DIRECTOR
BALLISTIC RESEARCH LABORATORIES
ABERDEEN PROVING GROUND, MD 21005
ATTN DRXBR-XA/MR. J. MESZAROS

COMMANDER
US ARMY AVIATION SYSTEMS COMMAND
12TH AND SPRUCE STREETS
ST. LOUIS, MO 63160
ATTN DRCPM-AAH/ROBERT HUBBARD

DIRECTOR
EUSTIS DIRECTORATE
US ARMY AIR MOBILITY R&D LABORATORY
FORT EUSTIS, VA 23604
ATTN SAVDL-EU-MOS/MR. S. POCILUYKO
ATTN SAVDL-EU-TAS(TETRACORE)

COMMANDER
2D BDE, 101ST ABN DIV (AASLT)
FORT CAMPBELL, KY 42223
ATTN AFZB-KB-SO/CPT PAUL C. SMITH

COMMANDER
US ARMY ELECTRONICS COMMAND
FT. MONMOUTH, NJ 07703
ATTN PM, ATACS/DRCPM-ATC/LTC DOBBINS
ATTN DRCPM-ATC-TM
ATTN PM, ARTADS/DRCPM-TDS/BG A. CRAWFORD
ATTN DRCPM-TDS-TF/COL D. EMERSON
ATTN DRCPM-TDS-TO
ATTN DRCPM-TDS-FB/LTC A. KIRKPATRICK
ATTN PM, MALOR/DRCPM-MALR/COL W. HARRISON
ATTN PM, NAVCOM/DRCPM-NC/
COL C. MCDOWELL, JR.
ATTN PM, REMBASS/DRCPM-RBS/
COL R. COTTEY, SR.
ATTN DRSEL-TL-IR/MR. R. FREIBERG
ATTN DRSEL-SA/NORMAN MILLSTEIN
ATTN DRSEL-MA-C/J. REAVIS
ATTN DRSEL-CT-HDK, ABRAHAM E. COHEN
ATTN DRSEL-CE, T. PREIFFER
ATTN DRSEL-TL-MD, GERHART K. GAULE
ATTN DRSEL-GG-TD, W. P. WERK
ATTN DRSEL-TR-ENV, HANS A BOMKE
ATTN DRSEL-TL-ME, M. W. POMERANTZ
ATTN DRSEL-TL-IR, ROBERT A. FREIBERG
ATTN DRSEL-WL-D
ATTN DRSEL-NL-D
ATTN DRSEL-TL-IR, EDWIN T. HUNTER
ATTN DRSEL-CT, RADAR
ATTN DRSEL-CT, RADAR DEVELOPMENT GROUP
ATTN DRSEL-WL, ELECTRONIC WARFARE LAB
ATTN DRSEL-CT-R, MR. BOAZ GELERNTER
ATTN DRSEL-WL-S, MR. GEORGE HABER
ATTN DRSEL-VL-G, MR. SOL PERLMAN
ATTN DRSEL-NL-CR-1, DR, FELIX SCHEVERING

COMMANDER
US ARMY MISSILE MATERIEL READINESS COMMAND
REDSTONE ARSENAL, AL 35809
ATTN DRSMI-FRR/DR. F. GIPSON
ATTN DRCPM-HA/COL P. RODDY
ATTN DRCPM-LCCX/L. B. SEGGEL (LANCE)
ATTN DRCPM-MD/GENE ASHLEY (PATRIOT)
ATTN DRCPM-MP
ATTN DRCPM-PE/COL SKEMP (PERSHING)
ATTN DRCPM-SHO
ATTN DRCPM-TO
ATTN DRSMI-R, RDE & MSL DIRECTORATE

COMMANDER
US ARMY ARMAMENT RESEARCH
& DEVELOPMENT COMMAND
DOVER, NJ 07801
ATTN DRDAR-ND-V/DANIEL WAXLER

COMMANDER
US ARMY TANK/AUTOMOTIVE MATERIEL
READINESS COMMAND
WARREN, MI 48090
ATTN DRSI-RHT/MR. P. HASEK
ATTN DRCPM(XM-L)/MR. L. WOOLCOT
ATTN DRCPM-GCM-SW/MR. R. SLAUGHTER

PRESIDENT
DA, HA, US ARMY ARMOR AND ENGINEER BOARD
FORT KNOX, KY 40121
ATTN STEBB-MO/MAJ SANZOTERRA

COMMANDER
WHITE SANDS MISSILE RANGE
WHITE SANDS MISSILE RANGE, NM 88002
ATTN STEWS-TE-NT/MARVIN SQUIRES

COMMANDER
TRASANA
SYSTEM ANALYSIS ACTIVITY
WHITE SANDS, NM 88002
ATTN ATAA-TDO/DR. D. COLLIER

COMMANDER
US ARMY COMMUNICATIONS COMMAND
FORT HUACHUCA, AZ 85613
ATTN ACC-AD-C/H. LASITTER (EMP STUDY GP)

DEPUTY COMMANDER
US ARMY NUCLEAR AGENCY
7500 BACKLICK RD
BUILDING 2073
SPRINGFIELD, VA 22150
ATTN MONA-WE/COL A. DEVERILL

COMMANDER
US ARMY SIGNAL SCHOOL
FT. GORDON, GA 30905
ATTN AISO-CID/BILL MANNELL
ATTN ATST-CTD-CS/
CAPT G. ALEXANDER (INTACS)
ATTN ATSO-CID-CS/LTC R. LONGSHORE

DIRECTOR
JOINT TACTICAL COMMUNICATIONS OFFICE
FT. MONMOUTH, NJ 07703
ATTN TRI-TAC/NORM BECHTOLD

COMMANDER
US ARMY COMMAND AND GENERAL STAFF COLLEGE
FORT LEAVENWORTH, KS 66027

COMMANDER
US ARMY COMBAT DEVELOPMENTS EXPERIMENTATION
COMMAND
FORT ORD, CA 93941

COMMANDER
HQ MASSTER
FORT HOOD, TX 76544

COMMANDER
US ARMY AIR DEFENSE SCHOOL
FORT BLISS, TX 79916
ATTN ATSA-CD

COMMANDER
US ARMY ARMOR SCHOOL
FORT KNOX, KY 40121
ATTN ATSB-CTD

COMMANDER
US ARMY AVIATION CENTER
FORT RUCKER, AL 36360
ATTN ATST-D-MS

COMMANDER
US ARMY ORDNANCE CENTER AND SCHOOL
ABERDEEN PROVING GROUND, MD 21005
ATTN USAOC&S
ATTN ATSL-CTD

COMMANDER
US ARMY ENGINEER SCHOOL
FORT BELVOIR, VA 22060
ATTN ATSE-CTD

COMMANDER
US ARMY INFANTRY SCHOOL
FORT BENNING, GA 31905
ATTN ATSH-CTD

COMMANDER
US ARMY INTELLIGENCE CENTER AND SCHOOL
FORT HUACHUCA, AZ 85613
ATTN ATSI-CTD

COMMANDER
US ARMY FIELD ARTILLERY SCHOOL
FORT SILL, OK 73503
ATTN ATSF-CTD

CHIEF OF NAVAL OPERATIONS
NAVY DEPARTMENT
WASHINGTON, DC 20350
ATTN NOP-932, SYS EFFECTIVENESS DIV
CAPT E. V. LANEY
ATTN NOP-9860, COMMUNICATIONS BR
COR L. LAYMAN
ATTN NOP-351, SURFACE WEAPONS BR
CAPT G. A. MITCHELL
ATTN NOP-622C, ASST FOR NUCLEAR
VULNERABILITY, R. PIACESI

COMMANDER
NAVAL ELECTRONICS SYSTEMS COMMAND, HQ
2511 JEFFERSON DAVIS HIGHWAY
ARLINGTON, VA 20360
ATTN PME-117-21, SANGUINE DIV

HEADQUARTERS, NAVAL MATERIEL COMMAND
STRATEGIC SYSTEMS PROJECTS OFFICE
1931 JEFFERSON DAVIS HIGHWAY
ARLINGTON, VA 20390
ATTN NSP2201, LAUNCHING & HANDLING BRANCH, BR ENGINEER, P. R. FAUROT
ATTN NSP-230, FIRE CONTROL & GUIDANCE BRANCH, BR ENGINEER, D. GOLD
ATTN NSP-2701, MISSILE BRANCH, BR ENGINEER, J. W. PITSENBERGER

COMMANDER
NAVAL SURFACE WEAPONS CENTER
WHITE OAK, MD 20910
ATTN CODE 222, ELECTRONICS & ELECTRO-MAGNETICS DIV
ATTN CODE 431, ADVANCED ENGR DIV

US AIR FORCE, HEADQUARTERS
DCS, RESEARCH & DEVELOPMENT
WASHINGTON, DC 20330
ATTN DIR OF OPERATIONAL REQUIREMENTS AND DEVELOPMENT PLANS, S/V & LTC P. T. DUESBERRY

COMMANDER
AF WEAPONS LABORATORY, AFSC
KIRTLAND AFB, NM 87117
ATTN ES, ELECTRONICS DIVISION
ATTN EL, J. DARRAH
ATTN TECHNICAL LIBARY
ATTN D. I. LAWRY

COMMANDER
AERONAUTICAL SYSTEMS DIVISION, AFSC
WRIGHT-PATTERSON AFB, OH 45433
ATTN ASD/YH, DEPUTY FOR B-1

COMMANDER
HQ SPACE AND MISSILE SYSTEMS ORGANIZATION
P.O. 96960 WORLDWAYS POSTAL CENTER
LOS ANGELES, CA 90009
ATTN S7H, DEFENSE SYSTEMS APL SPO
ATTN XRT, STRATEGIC SYSTEMS DIV
ATTN SYS, SURVIVABILITY OFC

COMMANDER
AF SPECIAL WEAPONS CENTER, AFSC
KIRTLAND AFB, NM 87117

HARRY DIAMOND LABORATORIES
ATTN RAMSDEN, JOHN J., COL, COMMANDER/ FLYER, I.N./LANDIS, P.E./ SOMMER, H./OSWALD, R. B.
ATTN CARTER, W.W., DR., TECHNICAL DIRECTOR/MARCUS, S.M.
ATTN KIMMEL, S., PAO
ATTN CHIEF, 0021
ATTN CHIEF, 0022
ATTN CHIEF, LAB 100
ATTN CHIEF, LAB 200
ATTN CHIEF, LAB 300
ATTN CHIEF, LAB 400
ATTN CHIEF, LAB 500
ATTN CHIEF, LAB 600
ATTN CHIEF, DIV 700
ATTN CHIEF, DIV 800
ATTN CHIEF, LAB 900
ATTN CHIEF, LAB 1000
ATTN RECORD COPY, BR 041
ATTN HDL LIBRARY (5 COPIES)
ATTN CHAIRMAN, EDITORIAL COMMITTEE
ATTN CHIEF, 047
ATTN TECH REPORTS, 013
ATTN PATENT LAW BRANCH, 071
ATTN GIDEP OFFICE, 741
ATTN LANHAM, C., 0021
ATTN CHIEF, BR 110
ATTN CHIEF, BR 120
ATTN CHIEF, BR 130
ATTN CHIEF, BR 140
ATTN CHIEF, BR 150
ATTN CHIEF, BR 160
ATTN CHIEF, BR 1010 (5 COPIES)
ATTN CHIEF, BR 1020 (5 COPIES)
ATTN CHIEF, BR 1030 (5 COPIES)
ATTN CHIEF, BR 1040 (5 COPIES)
ATTN CHIEF, BR 1050 (5 COPIES)
ATTN TOMPKINS, J. E., 230
ATTN WYATT, W. T., 1000
ATTN WIMENITZ, F. N., 0024
ATTN DROPKIN, H., 110
ATTN STARK, W., 1030
ATTN HEINARD W., 150
ATTN SCHAUBERT, D. (25 COPIES)